AD-A064 846 MICHIGAN UNIV ANN ARBOR DEPT OF NUCLEAR ENGINEERING F/G 20/9
LASER DIAGNOSTICS IN METALLIC PLASMAS.(U)
DEC 78 D R BACH AFOSR-74-2713

UNCLASSIFIED AFOSR-TR-79-0044 NL

END
DATE FILMED
4-79
DDC

FINAL REPORT

Laser Diagnostics in Metallic Plasmas

Period Covered: June 1, 1974-October 31, 1978

DAVID R. BACH

December 1978

Supported by:
United States Air Force
Office of Scientific Research
Grant No. AFOSR 74-2713
Washington, D.C.

College of Engineering
Department of Nuclear Engineering

THE UNIVERSITY OF MICHIGAN

COLLEGE OF ENGINEERING
Department of Nuclear Engineering

Final Report

LASER DIAGNOSTICS IN METALLIC PLASMAS

Period Covered: June 1, 1974 - October 31, 1978

David R. Bach

DRDA Project 012641

supported by:

UNITED STATES AIR FORCE
OFFICE OF SCIENTIFIC RESEARCH
GRANT NO. AFOSR 74-2713
WASHINGTON, D.C.

administered through:

DIVISION OF RESEARCH DEVELOPMENT AND ADMINISTRATION ANN ARBOR

December 1978

TABLE OF CONTENTS

ABSTRACT

The major objectives of the research described was the study of diagnostic techniques for metallic plasmas produced by exploded wire systems. Work accomplished included the development of a diamond die for the extrusion of lithium, ray tracing calculations to determine the deflection and absorption of rays passing through the plasma, and a transmission line calculation used for the design of etalons. Measurements made include X-ray temperature determinations by the line ratio method using scintillator detectors. Experiments were also carried out on a large area CdS detector for the measurement of infrared radiation.

A two-wavelength holographic interferometer was designed, constructed, tested, and used for the measurement of density distribution in the exploded wire plasma and a Z-pinch. The useful measurements were made with the system at the ruby doubled frequency, as the transmission through the plasma was greater at this wavelength.

The exploded wire system has been modified to accept solid wires of tungsten and aluminum which can be fed from outside the vacuum system and a new X-ray measuring system has been constructed.

A. INTRODUCTION

The major objectives of the research described was the study of diagnostic techniques for metallic plasmas produced by exploded wire systems. Work accomplished included the development of a diamond die for the extrusion of lithium, ray tracing calculations to determine the deflection and absorption of rays passing through the plasma, and a transmission line calculation used for the design of etalons. Measurements made include X-ray temperature determination by the line ratio method using scintillator detectors. Experiments were also carried out on a large area CdS detector for the measurement of infrared radiation.

A two-wavelength holographic interferometer was designed, constructed, tested, and used for the measurement of density distributions in the exploded wire plasma and a Z-pinch. The useful measurements were made with the system at the ruby doubled frequency, as the transmission through the plasma was greater at this wavelength.

Single wavelength holographic interferometry was applied to the study of an exploding lithium wire plasma. The wire was 1 mil in diameter, extruded in vacuum. A holographic quality ruby laser probe produced a 15 ns FWHM pulse at $\lambda = 694.3$ nm with 45 mJ in the TEM_{00} mode. A temperature controlled resonant reflector restricted laser operation to essentially a single longitudinal mode. Linear charge density measured from Abel inverted interferograms implied that a significant amount of neutral or unionized lithium was present in a cold core. Peak electron density reached 1.4×10^{19} e^-/cm^3 and $2 \text{ eV} < T_e < 10 \text{ eV}$, but significant neutral contribution prevented accurate electron density determination near the core. Three characteristic periods of plasma development were identified and compared to time resolved streak photographs of the luminous plasma front and optical spectra. Of special interest, a period of localized neutral "cloud" formation was observed with densities reaching 8×10^{17} cm^{-3}, forming after self-pinching and before peak discharge current.

The exploded wire system has been modified to accept solid wires of tungsten and aluminum which can be fed from outside the vacuum system and a new X-ray measurement system has been constructed.

This report contains descriptions of the items mentioned above. Although a large part of the material has been, or is being, reported in the open literature, all of the significant results are reported here for completeness.

B. HOLOGRAPHIC INTERFEROMETRY

Exploding wires have been studied for years as X-ray sources, detonation fuses, shock sources,[1,2] and as sources of high density plasma for laser-plasma coupling experiments.[3] Theoretical modeling of the plasma spectroscopic, electronic, and MHD characteristics required detailed knowledge of the radial electron density profile across the plasma column. With such knowledge one can ray trace through the known profile and predict absorption along the path.[4] Spectral emissivity can then be estimated, electronic characteristics can be explained, and MHD models can be verified.

The steep density gradients ($> 10^{20}$ cm^{-4}) and high peak electron densities (10^{18}-10^{19} cm^{-3}) of exploding wire plasmas restrict the techniques of density profile measurement to optical interferometry. Since exploding wire plasmas of high energy density are infamously irreproducible, an entire profile measurement must be made in one shot. By choosing a laser of sufficiently small pulsewidth, but sufficiently large energy one can freeze plasma motion and illuminate the entire plasma in one arm of an interferometer. Optical interferometry of the Jamin or Mach-Zehnder type requires high optical quality windows, lenses, and reflecting surfaces. Double-exposure holographic interferometry does not have such limitations, and was utilized in this investigation of exploding lithium wires.

Holographic interferometry has been successfully utilized elsewhere to provide high temporal and spatial resolution of fully ionized, high density plasmas.[5-7] Exploding wire plasmas, however, are rarely fully ionized and present a formidable challenge to quantitative electron density measurement. Two-wavelength interferometry is specifically equipped to solve this problem by eliminating the neutral contribution to refractivity.[8] Much two-wavelength work appears in the literature.[6,9,10] but little of it is applied to partially ionized plasmas. In one particular case two-wavelength holographic interferometry was applied to exploding wire plasmas with rather uncertain results.[11]

Single wavelength holographic interferometry still holds the possibility of obtaining qualitative information regarding temporal plasma development and hydrodynamic stability. It also permits estimation of the level of ionization, which may be compared to computed estimates based on a matrix of equilibrium rate equations. Neutrals in a partically ionized plasma contribute both to refractivity and to absorption. They not only increase the ambiguity of interferometric measurements, but they may destroy fringe contrast by decreasing the transmitted beam intensity in the interferometer object arm.

The primary experiments performed to date in holographic interferometry of exploding wire plasmas have been those of J. L. Seftor.[11,12] In his publications Seftor commented that improved laser spatial behavior would significantly improve the quality of his holograms.

In the work described in this article, a KORAD ruby laser has been modified to produce a unitorm TEM_{oo} output mode of 45 mJ energy and 16 ns FWHM pulsewidth. This holographic quality laser has been utilized to generate holographic interferograms of a 1 mil (25 μm diameter) exploding lithium wire plasma. The study has revealed much in terms of wire plasma dynamics and effective charge state.

Holographic interferograms were produced with a double-exposure, image-plane technique. Referring to Figure 1, a ruby laser operating at 694.3 nm generated a 2.0 nm diameter TEM_{oo} beam, which was expanded via lenses L_1 and L_2 to 7 cm diameter. The reference beam was collimated and directed via beam-steering mirrors (not shown in Figure 1) to the holographic data. KODAK 120-02 plates were used throughout. The object beam was collimated and directed through the vacuum chamber containing the 5-cm long, 1-mil diameter lithium wire. The exploding wire plasma was imaged 1:1 onto the holographic plate in order to capture refracted rays. A 50-cm focal length, 6.3 cm diameter lens was used for imaging. This permitted the observation of electron density gradients reaching 7×10^{20} cm^{-4} over the entire plasma radius during a pinch. Between the two laser exposures, one of the reference beam-steering mirrors was rotated. This changed the incident reference beam angle by ~ 1.7 mrad and placed moiré fringes on the interferogram spaced 4 to 5 lines/nm. Neutral density filters in the interferometer arms adjusted exposing intensity to achieve a final exposed density of ~ 1. The laser and beam expanding optics were floated on inner tubes to maintain laser mirror alignment, but all other components were hard mounted.

High holographic diffraction efficiency was obtained by insuring single or adjacent longitudinal mode laser operation and TEM_{oo} transverse mode operation. Spatial coherence was further maintained by selecting better quality vacuum chamber windows (i.e., windows of high optical finish as observed by the eye) and by avoiding inhomogeneous regions of optical filters. An intracavity aperture restricted oscillation to the lowest order transverse mode. Longitudinal mode control was obtained by replacing the normal output sapphire etalon with a BK-7 four-surface resonant-reflector. The reflector was placed within a temperature controlled oven steady to ± .01°C. The measured interferometer coherence length was .8 meter, implying a lasing bandwidth of .0025 Å (when frequency sweep during the pulse is taken into account).[13] This corresponds to one axial mode oscillating strongly and one adjacent axial mode oscillating weakly in the 75-cm laser cavity.

The exploding wire plasma was initiated by discharging a 13.7 μf, 40 nH capacitor charged to + 15 kV through a 1 mil diameter lithium wire. The wire was extruded through a diamond die in a vacuum of 5×10^{-6} torr, insuring no oxygen or hand oil contamination (see Figure 2). Peak current reached 100 kA with a quarter ringing period of 3.25 μs. (The eletrical charging and triggering circuit has been presented elsewhere.[3]) A streak camera viewed the plasma at 90° to the interferometer object arm, monitoring the plasma luminous front with an S-20 response photocathode. Streak photographs were compared

with observations of di/dt through the plasma, as observed on a Rogowski coil (where i = current and t = time).

Earlier spectroscopic studies of this exploding lithium wire plasma had placed electron densities in the range of 2 to 6×10^{18} cm^{-3} (via Stark broadening) and electron temperatures in the range of 2 to 10 eV (via line-to-line and line-to-continuum ratios).[3,14] The only prior study of the electron density profile was qualitative and indicated the presence of a cold, poorly ionized neutral core.[3] Together with streak photographs, spectroscopic, and di/dt data, a picture had been formed of a dense, partially ionized, cold plasma whose radius would pinch down at unpredictable times before peak current was attained. During a pinch caused by self-generated B-fields, electron density and temperature rose and anomalous dips in di/dt resulted from changes in plasma inductance. Spectra and streak photographs only viewed a small linear segment of the exploding wire, and one could not confidently extrapolate these findings to the entire plasma length. Holographic interferometry promised to fill this gap and to provide electron density profile information and MHD stability information over the entire wire length.

Reconstructed interferograms revealed significant temporal and spatial details of our exploding wire dynamics. The sausage or m = 0 instability was seen to occur, although early plasma column dissembly did not usually result. Significant variations in plasma column diameter were observed over short distances, indicating nonuniform lithium extrusion. Peak electron density, however, remained fairly uniform along the plasma column axis in spite of local radial variations. For ease of discussion the axis of symmetry of the plasma column will be termed the z-axis.

Three principle periods of exploding wire plasma development were studied interferometrically. These periods follow the initiation of current flow through the lithium wire at time = t_o.

A. Most profound self-pinching occurred between t_o + 1.0 μs and t_o + 1.8 μs. Such rapid reductions in plasma radius were easily observed in streak photographs and often corresponded to dips in di/dt. An interferogram taken during a pinch at t_o + 1.0 μs is shown in Figure 3. The 2.4-mm diameter turbulent region at the base of the plasma shows the influence of the lower electrode on plasma formation. Clearly holographic interferometry identifies scientifically usable regions of the wire plasma. While pinching does appear to occur over the entire length, absolute plasma radii vary along the z-axis. This implies a nonuniformly extruded wire in spite of the hard diamond die.

Electron density is indicated by the rate of fringe shift as the fringe enters the plasma. This rate varies significantly along the z-axis and indicated the presence of an m = 0 instability. A close inspection of the interferogram of Figure 3 reveals the lack of fringe penetration through the core of the plasma. Density profiles were measured at two z-positions along the plasma. One profile was measured at the very narrow region near the top of the interferogram, where a fringe completely penetrates the plasma. A second

profile was measured 0.75 cm below this. The fringe shifts were Abel inverted and plotted in Figure 4. The profile indicated by the circles was measured in a region where fringes did not penetrate the core. The significant variation in radial profile at different points along the z-axis has been interpreted as being caused by the nonuniform wire extrusion.

The extent of ionization may now be directly calculated. The linear atom density (#/cm) is known from the initial lithium wire diameter. The linear electron density may be calculated from Figure 4 by integrating under the curve over the differential area element $2\pi r dr$, where r = plasma radius. The integration reveals an effective charge, Z_{eff} of 0.55. Computations based on Saha equilibrium and on equilibrium rate equations both predict $Z_{eff} = 1.0$ for electron temperatures above 1.5 eV. The low apparent effective charge results from the contribution of neutrals to the index of refraction, resulting in a reduced phase shift through the medium.

The interferometrically measured phase shift of a straight-line ray through the circular cross-section plasma may be expressed as

$$\Phi = \int_0^L \left(\frac{2\pi}{\lambda}\right) [\eta(r) - 1] \, d\ell \quad , \tag{1}$$

where Φ = phase shift

L = straight-line path through the plasma

λ = laser probe wavelength

$\eta(r)$ = index of refraction as a function of radius

and

$d\ell$ = differential physical pathlength

$\eta(r)$ for neutrals varies only weakly with λ and the phase shift Φ essentially varies as λ^{-1} and is positive in sign. The electron index of refraction is always less than one and varies with λ^2. Thus, the electron contriburion to Φ varies as λ and is negative in sign. A neutral density of 2×10^{18} Li atoms/cm^3 would contribute equally to refractivity (but in the opposite direction) as would an electron density of 1.5×10^{19} e$^-$/cm^3 at λ = 694.3 nm. Small neutral concentrations can seriously reduce measured fringe shifts. This in turn reduces the calculated electron density profile, if only electrons are assumed to contribute.

The presence of neutrals could be expected to have caused the loss of fringes in the core region, r < 0.013 cm. Photoionization losses in this cool lithium plasma could account for 30% absorption across a 0.2 cm path.[15] This loss could reduce front visibility and along with small scale turbulence eliminate observed fringes in the core.

A 1-D single fluid, two temperature MHD code with equilibrium rate equations was run to predict wire plasma dynamics. It showed a very peaked structure in the electron density profile away from the z-axis during a pinch (see Figure 5). The drastically reduced interior electron density may be alternatively interpreted as a region of a low level of ionization.

The picture of the pinched exploding wire plasma consisting of a warm exterior and a cool, poorly ionized interior appears confirmed.[3] Electron temperature inferred from the Bennett relation yields 27 eV for $Z_{eff} = 0.55$ and 19 eV for $Z_{eff} = 1.0$. Since spectra confirm lower temperatures, a higher Z_{eff} is supported. A refraction code was run to insure that lost fringes could not be due to steep gradients. All angles of refraction should have been caught by the imaging lens.

B. The second time period of interest occurred between t_o + 1.8 μs and t_o + 2.1 μs. During this time current was still rising through the electrical circuit and had reached ~ 80 kA. Streak photographs revealed a wide, diffuse illuminated region with no further pinching taking place. Figure 6 is a reconstructed interferogram taken during this period. It reveals the surprising presence of a cloud of neutrals, condensed within a background of a broad, low-density plasma. Such clouds were consistently observed at these times as evidenced by fringes which were shifted downward, opposite to fringes shifted by electrons.

An Abel inversion through the center of the neutrals produced the profile seen in Figure 7. The index of refraction for LiI was computed via the Lorentz-Lorenz formula.[16] The microscopic polarizability at 694.3 nm was calculated from the LiI transitions and oscillator strengths found in the NSRDS-NBS 4 tables.[17,18] Surprisingly low densities are seen in the cloud, considering the amount of fringe shift measured. A calculation of linear density in this cloud shows that only 5% of the original linear density is present. That is, 95% of the original lithium is outside the condensed region.

The presence of the neutral clouds has two possible explanations. Adiabatic cooling of the plasma may occur as it rapidly expands following a pinch. A simpler explanation, however, is that the core was never ionized and joule heating occurred primarily on the wire surface. This latter explanation is supported both by (1) classical electromagnetism, which would imply an exponential current penetration of the wire, due to the fast rising external circuit turn-on, and (2) MHD computations of the current density as a function of plasma radius, showing a decrease with decreasing radius.

C. The final interesting stage of exploding wire plasma development occurred between t_o + 2.4 μs and t_o + 2.6 μs. Interferograms taken in this period finally show the broad, diffuse plasma that one would expect, sans neutrals; current has reached 93.5 kA, near its peak value. The plasma appears as a hoop expanding outward at a radius of 0.5 cm. The simultaneous observation of a strong 610.4 nm neutral lithium line implies a low level of ionization with the current being shunted along the outermost regions of the plasma.

Single wavelength holographic interferometry of a 1 mil exploding lithium wire plamaa was able to provide valuable information on plasma dynamics and ionization state not available with streak photography. However, it was limited in quantitative data extraction because of the unique mix of neutrals and electrons. Neutral refractivity and absorption prevented complete interferometric analysis of the partially ionized lithium plasma.

Confirmation was gained of several previously unclear phenomena. It was learned that a pinch as observed in a streak camera corresponded to a reduction in radius along the entire z-axis of the wire, not just the portion observed in the streak camera. Pinches did, in fact, correspond to dips in di/dt. In spite of the hard diamond die, pinching was nonuniform, implying a nonuniform extrusion.

Electron densities exceeded 1×10^{19} cm^{-3} in the pinch with gradients of $\sim 6 \times 10^{20}$ cm^{-4}. More accurate measurements were precluded by the presence of neutrals.

Shortly following pinches, localized clouds of neutrals have been observed in the midst of a low density plasma. Neutral densities reached 8×10^{17} cm^{-3} and existed at a time when the current was 80 kA. No similar reports have been made in the literature of exploding wires.

Comparison to exploding wire work at other laboratories was not possible, because of widely varying experimentaal conditions. The closest work was that of L. Seftor, who has performed holographic interferometry of exploding wires at 694.3 nm, and at 694.3 and 347.2 nm.[11,12] His energy density was lower with a peak current of 14 kA and a charging voltage of 15 kV, and his circuit was approximately three times faster than ours. His two-wavelength interferometry showed a greater sensitivity at 347.2 nm than at 694.3 nm (unless the spatial scale differed between his interferometric reconstructions). This implied that he was viewing neutrals rather than electrons, since electron refractivity decreases as wavelength decreases as discussed earlier in this article.

C. RAY TRACING THROUGH A COLD, COLLISIONLESS PLASMA

Optical absorption and scattering experiments in high density plasmas may be subject to significant refractive losses. This problem becomes especially important when probing the plasma with light at frequencies approaching the critical frequency. (Our plasmas cover the density range of 10^{18}-10^{19} cm^{-3} and the critical density for 10.6 μm CO_2 laser light is 10^{19} cm^{-3}.) To account for energy lost via refraction we have successfully solved the problem of tracing a ray of light through a cylindrically symmetric, cold, collisionless plasma. We generated a computer code which numerically solves for the angle of refraction as a function of "impact parameter" (in analogy to scattering theory) for any given radial electron distribution. The program also calculated absorption along the path allowing us to compute the expected energy distribution of refracted light around our cylindrical Z-pinch and exploding wire plasmas.

The formula of Bouguer (cf. Born and Wolf, Principles of Optics) was utilized as the starting point for this analysis. Bouguer's result is depicted in Figure 8 and says that the product $N \cdot r \cdot \sin \varphi$ is constant along a ray path in any cylindrically symmetric medium. (N = index of refraction, r = distance from origin to the point of interest, φ = angle between $\underline{r}$ and the tangent to the ray at $\underline{r}$.) The plasma geometry presented in Figure 9 permits treatment of the problem as one would a scattering problem, looking for the scattering angle or refraction angle as a function of impact parameter. This same figure reveals $N \cdot r \cdot \sin \varphi$ evaluated at the radius to be C, the impact parameter. RB, the distance of closest approach, may now be readily computed given a particular density distribution. The angle φ and the polar coordinates r and θ may be related as in equation (1) in Figure 10. Using the formula of Bouguer one arrives at an integral expression for the angle $\Delta\theta$ traversed by the ray as it passes from the outer radius R to RB. By symmetry the total polar angle traversed will be $2\,\Delta\theta$. It should be noted paranthetically that Fermat's principle could also have been used to produce equation (3).

Take note of the singularity in the integrand of this last equation. When evaluated at the distance of closest approach, RB, NR = C, and the denominator goes to zero. Solving this integral then becomes the primary obstacle to obtaining a tractable expression for the refraction angle. Rather than wave our hands as r approaches RB we found integration by parts provided a most elegant solution. We first note in Figure 11 that the denominator may be split into the product of a sum and difference, only one term of which is singular. By carefully choosing U and V of the parts integration, the singularity may be raised out of the denominator. This process results in a lengthy, but readily manageable expression as seen atop Figure 12.

Equation (4) is expressed in terms of normalized radius x. Limits run from RB/R to 1 rather than from RB to R. The expression for du/dx consists of three terms, each of which is similar structurally to the first term in equation (4), but which contain both first and second derivatives of the index of

refraction. Solution for $\Delta\theta$ is straightforward. Choose a likely density distribution and determine the index of refraction N in terms of this distribution. Then find the first and second derivatives of N with respect to x. Now we can program this expression for $\Delta\theta$ and solve numerically producing a solution for Ω_p, the angle of refraction. A similar integral solution may be obtained to determine the total path length traversed in the plasma. Thus absorption along that path may also be computed.

The results of these calculations show the refraction angle to be a peaked function of the impact parameter (assuming a parabolic e^- density distribution) rather than a monotonic function. Such a plot is seen in Figure 13 where the optical probe chosen was 10.6 μm with a critical density of 10^{19} electrons/cm^3. As MD approaches one, the peak density at the origin approaches the critical density. Note that significant refraction angles should be expected when on-axis electron densities exceed one-third of critical density. Alternatively one could use a measurement of refracted light to work back and infer peak electron densitities assuming some knowledge of the radial distribution. Absorption calculations based on the same distribution as Figure 13 and utilizing free-free inverse bremsstrahlung as the absorption mechanism revealed strong absorption for all ray paths when peak densities exceed one-third critical density.

The analytical work done here was quite original. Fermat's principle has been used by others to generate a first-order partial differential equation, which they then solve by using a Crank-Nicholson or similar numerical analysis scheme. F. Keilman of the Max-Planck Institute used Bouguer's formula,[33] but failed to solve the resulting integral and instead linearized his equations and solved for small refraction angles—missing much of the most useful information. Our solution is as accurate as the numerical technique without the associated numerical stability problems. Combined with an interferometric determination of radial density profiles, this program will prove highly valuable in (1) assessing refractive contributions to scattered laser energy, (2) further reducing experimental error in absorption measurements, and (3) providing another diagnostic for density measurements in dense plasmas.

D. ABEL INVERSION PROGRAM

The holographic measurement yields phase shifts of the laser radiation which passes through the plasma. A computer program has been written to determine the density of the plasma as a function of radius, by performing an Abel inversion 6 of the phase drift data.

A major part of the program involves performing the following integral:

$$f(r) = -\frac{1}{\pi} \int_r^{r_o} \frac{f_A'(x)dx}{(r^2 - r^2)^{1/2}} \qquad (2)$$

where $f_A(a)$ contains the input data known only for discrete values of x. The portion of the program which evaluates this integral is itself divided into several portions. Each portion of the program and the program as a whole were verified using test data which could be evaluated analytically, thus determining the accuracy of the calculation. The first portion of the program fits the data with a cubic spline and hence provides a means of interpolating between data points. This spline consists of cubic polynomials which fit the data for each interval of data and are chosen such that the piecewise cubic function has a continuous first derivative. The second portion of the program calculates F f'(x) based on the values of $f(x + \delta x)$ and $f(x - \delta x)$ provided by interpolations. f'(x) is calculated at the values of x demanded by the third portion of the program. The third portion of the program evaluates the integral (2) using the trapezoidal rule together with Romberg's extrapolation method.

The calculation as a whole is accurate to approximately 1%. This accuracy is sensitive to the input data. Functions which vary slowly for values of x slightly larger than r are especially subject to error, since errors in the calculation of f'(r) are relatively large and are weighted heavily. For such functions, the program output must be examined closely, and the lower input limit of integration must be increased from the value r to some value $r + \delta r$ for which f'(x) is well defined.

E. DESIGN OF A FOUR-SURFACE RESONANT-REFLECTOR: APPLICATION OF TRANSMISSION LINE THEORY TO OPTICAL RESONATOR ANALYSIS

A four-surface resonant-reflector was chosen as the best means of increasing the coherence length of our ruby laser to aid in performing holographic interferometry. The reflector narrows the bandwidth of the output laser light by acting as a variable reflectivity output coupler, replacing the laser front mirror. The design of the reflector or complex etalon entailed choosing the thickness of the two glass plates involved, their spacing from one another, and determining the proper index of refraction of the glass. The front and rear surface of each plate comprising the reflector act as a series of dielectric surfaces from which reflection and transmission will occur. Näive solutions for the E-field components of a normally incident wave result in a tedious series of matrix multiplications (cf. Born and Wolf, Principles of Optics) and is the approach taken by many.[19-21] A more physically appealing approach was to utilize the concept of impedance and impedance matching at a boundary. We treat each interface or each surface as an impedance characterized by a particular permittivity and then transform that impedance back down the line towards the source to find the "effective" input impedance. This final impedance contains all the information about the multiple reflections between interfaces, and the series of resonant cavities appears as a transmission line.

Kirchoff's laws applied to a distributed parameter analysis of a transmission line yield wave equations for the voltage and current called the telegrapher's equations. These are expressed in the upper half of Figure 14 with a sinusoidal time dependence assumed. V_+ and V_- refer to the incident and reflected waves, respectively; Z_o is the characteristic impedance of the line, and β is the propagation constant. Similarly, if we assume we have a plane, polarized wave traveling in the z-direction in a linear, homogenous lossless medium without sources, this also yields a wave equation whose solutions may be expressed as in the lower half of Figure 14. We define η as the characteristic impedance of the medium and frequency information is carried out in K, the propagation constant. The analogy is continued in Figure 15. As the reflection coefficient is V_+/V_- in the transmission line case, so we deine it in terms of η in the plane wave case. (Note: load impedance, $Z_L \equiv \frac{V_+ + V_-}{I_+ - I_-}$). The input impedance Z_{IN} at a distance L back from a dielectric interface is computed at the bottom of thie figure. Here L_1 represents the optical path length in the medium.

In Figure 16 the entire process is diagrammed. Assuming light incident from the left, the characteristic impedance of each medium is given by η; its thickness by L. We compute the input impedance at the n-1:n-2 interface by transforming η_n back through L_{n-1} and so on until we compute the effective input impedance at the first air-dielectric interface. Then the amplitude reflection coefficient is simply given as Γ_{total}. Wavelength information is

carried in the propagation constant. Thus by starting with the first expression for input impedance and iterating through the dielectric stack we can arrive at an expression for reflectivity as $|\Gamma_{total}|^2$, a function of wavelength, index of refraction, and dielectric thicknesses. By programming the impedance transformation in a simple DO-loop, we can compute reflectivity at a given wavelength—then increment wavelength. The code written here accepts as input (1) number of dielectrics, (2) starting λ, (3) index of refraction of the jth dielectric, and (4) physical thickness of the jth dielectric. It then plots reflectivity as a function of wavelength.

The earliest mention of the use of a four-surface resonant reflector was by Hercher at Rochester in 1965.[22] By passive Q-switching he achieved repeatable single-mode oscillation. At the same time Sooy reported that mode selection is enhanced as giant pulse build-up pulse build-up is slowed. If we assume the primary loss mechanism to be the variable reflectivity of the front resonator then we can account for gain differentiation between modes in Figure 17. The more loop transits of the cavity, the greater the gain differentiation between modes. Note the great difference in Q for Pockels type Q-switch vs. a passive switch. From use of our code RESONATOR a design was chosen utilizing BK-7 glass plates 2 mm thick separated by 30 mm. This design achieved the optimum spectral characteristics by allowing at most two axial modes to oscillate simultaneously.

F. LINE TO CONTIMUUM TEMPERATURE MEASUREMENT

Previous studies in this laboratory have shown intense continuum radiation emanating from the exploded wire plasma during the time of plasma contraction, or "pinch," time. Computer calculations of the plasma dynamics have indicated the electron temperature at these times to be between 10 and 40 eV. Our standard line ratio temperature measurements were not usable and therefore most of our experiments were done at plasma temperatures of about 5 eV. As the electron densities in the "pinch" are expected to be about 10^{19} per cm^3, the critical density for CO_2 laser radiation, this is an extremely interesting region to study.

In an attempt to understand this part of the plasma, an experiment was devised to extract the temperature. A wide-band spectrometer was used (> 2000 Å) in conjunction with an NBS calibrated tungsten filament, an improved microdensitometer (range 0 to 1.3 density), and an improved optical imaging system to allow a faster streak (2 μs as opposed to 20 μs).

With the improved equipment, we found that all continuum regions still had lines which could be extracted. This discovery was the result of an improved microdensitometer which showed that earlier photographic studies were using overexposed films in the continuum region Analysis of these lines showed the following:

1. Temperature at "pinch" time were about 10 eV; in the line region immediately prior to a pinch the plasma was found hotter than in the middle of the line region (between pinches).

2. Densities were found to be about 5×10^{18} cm^{-3}.

3. Agreement was found between line ratio and line to continuum estimates of temperature. Again, this was the result of improved microdensitometer tracings. This indicated the likelihood of LTE between external and internal degrees of freedom.

X-RAY DIAGNOSTICS OF EXPLODING WIRE AND Z-PINCH

Previous investigation in this laboratory has indicated that at the time of pinching in the exploding wire plasma, spectral lines are overwhelmed by continuum plasma light emission, mkaing temperature determination by ratios of line intensities at the time of pinch quite difficult. This emission, due to acceleration of free electrons in the coulomb field of lithium ions, gives rise to the bremsstrahlung continuum, whose spectral distribution, is a well-known function of electron temperature.[24] By examining the spectral distribution in the energy regime above the last ionization potential for lithium, only this bremsstrahlung emission is seen.

As a pilot study to determine whether X-ray energy sufficient for diagnostics was emitted from the lithium exploding wire plasma, an X-ray detector was contructed utilizing the principles outlined by Jahoda and others.[25] The detector (Figure 18) was composed of a thin (5 to 35 mg/cm^2) aluminum foil window followed by a thin-film (1.02×10^{-2} cm) plastic scintillator (NE-102) optically coupled to the entrance window of a photomultiplier tube (RCA-8575). A certain portion of the X-ray spectrum emitted from the plasma, as determined by the absorption cross-section and thickness of the foil window and the thin-film scintillator, entered the plastic scintillator. By displaying the output of the photomultiplier tube which temporally resolved X-ray emission to better than 35 nsec, a record of X-ray emission versus time was obtained. Furthermore, by changing window thickness and/or material, energy information was obtained and was related to the electron temperature of the plasma. Just behind the foil entrance window to the detector was placed a 300 G magnet to reflect any charged particles that might enter the scintillator. The interior of the detector was evacuated to a pressure of less than 20 milliTorr to prevent attenuation of X-rays on the way to the detector.

To interpret the results and provide energy information, a computer code, KXRAY, was devised. The pulse height from the detector, $W(T,t)$, where T is the plasma temperature and t is the foil thickness, resulting from X-rays of spectral distribution $X(E,T)$ was determined by the transmission of the foil, $F(E,t)$, the stopping power of the scintillator, $G(E)$, and the light output of the scintillator for incident X-rays of energy E, $S(E)$. More specifically,

$F(E,t) = \exp(-\sigma(E)t)$; $\sigma(E)$ - absorption cross section as function of energy for the foil used

t - thickness of foil

$G(E) = 1 - (\exp(K(E)x))$; $K(E)$ - photoelectric cross section of scintillator

x - thickness of scintillator

$S(E) = \alpha E$; α - number of electrons emitted from photocathode of PM tube per one 1-keV X-ray

The foil absorption cross section, $\sigma(E)$, was represented as a straight line on a plot of log σ versus log λ, where λ is the wavelengtn associated with an X-ray of energy E:

$$\log \sigma = \log \lambda + \eta$$

To account for the discontinuity of the K-edge (at 1.55 keV in aluminum), a discontinuous change in η at the edge energy was accounted for A similar bilinear representation was used for calculating K(E) to obtain G(E). The linear treatment of the scintillator-photomultiplier tube response in arriving at S(E) has been found to be accurate, even at these low photon energies.[26] The product F(E,t)G(E)S(E) defined a detector response function, H(E), which can be viewed as the relative pulse size from the detector for an X-ray of energy E incident upon the foil (Figure 19). The output of the detector, W(T,t), is the product of the detector response function, H(E), and the bremsstrahlung spectral distribution function, X(E,T), integrated over all energies. For high energies compared to the final ionization potentential, X(E,T) is proportional to exp(E/kT), where k is Boltzmann's constant. The program KXRAY computes $W(T,t) = \int_0^\infty dE H(E,t) X(E)$ by Romberg integration for two thicknesses of foils for a given temperature and found the ratio of W(T,t) for the two foils. Thus, a plot of $R(T) = \frac{W(T,t)}{W(T,t')}$ versus temperature for a number of foil combinations was made so that an experimentally determined ratio could be associated with an electron temperature (Figure 30). Furthermore, an absolute X-ray energy emission calculation was performed using W(T,t) and included plasma density, volume, charge state, and solid angle viewed by the detector (Figure 21). Such a calculation is not as credible as a ratio determination, as the quantities which cancel out in a ratio measurement are not easily determined.

We found that X-rays were observed by the detector from the exploding wire in sufficient quantities to saturate the detector for window thicknesses of less than 27.4 mg/cm^2 of aluminum. These X-rays occurred in pulses having full-widths of 50 nsec at times of sharp dips in the time derivative of the current through the plasmas, dI/dt (Figure 22). By using X-ray detector signals for 27.4 mg/cm^2 and 34.3 mg/cm^2 aluminum foil windows, a determination of electron temperature at time of pinch was attempted. Since only one detector was constructed for this pilot study, measurements with different foil thicknesses had to be made on different shots, which depended upon the rather tenuous assumption that the evolution was reproducible from shot to shot. By averaging together several shots at each of the two foil thicknesses, a ratio value of 12.5 was used, although shot-to-shot variation gave a range of ratios

from 10.4 to 13.0. This yielded an electron temperature at time of pinch 75 eV, ranging from 70 to 155 eV (Figure 20).

Having verified that sufficient X-ray emission occurs from the exploding wire plasma to provide a useful diagnostic, further work will include using a two-detector system to measure the temperature more accurately and as a function of time as the pinch evolves. To verify that the emission has occurred from a Maxwellian distribution, several ratio measurements will be made with a wider range of foil thicknesses. If all ratios indicate the same temperature, one may believe that the X-ray spectrum was indeed Maxwellian. The investigation has suggested that enough X-rays must be present for imaging with an X-ray pinhole camera.

Having verified detector operation by observing X-rays from the exploding wire, we modified the X-ray detector to fit onto one of the four arms of the Z-pinch target chamber to determine whether an X-ray continuum was emitted by the Z-pinch plasma. This was done by removing the tube between the foil window and the scintillator shown in the right portion of the drawing of the detector, moving the foil window much closer to the scintillator and photomultiplier tube. Unfortunately, since the detector was closer to the Z-pinch discharge than it was to the exploding wire, the detector became a path to ground for the discharge current, impeding evolution of the plasma and producing very puzzling signals on the detector output. To prevent this, the brass detector case was subsequently isolated from ground by minor redesign and re-insulation.

We looked for X-ray emission from the Z-pinch plasma using aluminum foil windows ranging from 1.65 mg/cm^2 to 9.40 mg/cm^2. We also attempted to make our own absorbers, more transparent to low-energy X-rays, by evaporating 100 to 1000 nm of aluminum on 1.4 mg/cm^2 polyethylene. This proved unsuccessful, as after evaporation, the aluminum layer was marred with small pinholes which allowed light from the discharge to reach the photomultiplier tube, giving a false indication of X-rays.

To further lower our temperature detection threshold, then, we purchased some beryllium foil (4.7 mg/cm^2 and 2.3 mg/cm^2) for use as the X-ray window. The beryllium was quite brittle and one foil was slightly damaged by acoustic shock from the discharge.

Initial results were plagued by light leaks in the foil and pickup of electromagnetic noise from the discharge. The leaks and noise gave the misleading impression that X-ray bursts were emitted. As a control check, we selectively blocked X-ray wavelengths from the detector, but not optical wavelengths by covering the foil window with glass of sufficient thickness to block X-rays up to 15 keV. The subsequent Z-pinch shots, since they yielded detector pulses similar to those previous, indicated that plasma light and electromagnetic interference were giving false indication of X-ray pulses.

To reduce the appearance of electromagnetic interference from the discharge on the detector output, the high-voltage power supply for the detector was moved away from the discharge and placed in the shielded screen room with the timing electronics. Also, additional shielding was placed on the detector, and the signal wire within the detector was replaced with shielded 50 Ω cable. In addition, a method of visual inspection was developed that allowed detection of pinholes as small as 5 μm diameter.

Subsequent experiments with the foils mentioned indicated no X-ray emission from the plasma within the energy domain of our detector. Using the absolute calibration estimate described earlier, the results indicated an upper electron temperature bound of 40 eV. This upper limit is reinforced by a Bennett relation calculation of electron temperature for an equilibrium pinch, and by a laser probe absorption experiment, both of which indicate temperatures lower than this.

We looked for X-ray continuum from the plasma when the high-intensity CO_2 laser was incident. The focal volume of the laser was much smaller than the portion of the plasma viewed by the detector, so a large temperature increase, about 200 eV, was needed in the focal region before any observation of X-ray continuum was expected. No X-rays were observed in these experiments, again providing an upper bound in temperature, but no insight into heating.

Generally, even the lack of observable X-rays proved to be useful information, as it allows an opper limit in temperature to be set on the Z-pinch plasma. This knowledge of a low temperature is very important in our present work in CO_2 radiation - plasma interaction experiments, as it allows us to match some experimental conditions of the large laser-fusion laboratories with a more modest laser power requirement.

H. LARGE AREA DETECTOR STUDY

There continues to be a considerable problem in the study of the intensity distribution of 10.6 μ radiation as a function of space at intenstities too low for the use of exposed polaroid film and thermal sensitive paper. Although the liquid crystals are more sensitive, the procedure which makes use of normal photography of a liquid crystal does not provide the time dependent information which one would like to obtain due to the slow response of the liquid crystal.

In order to make use of the greater sensitivity of the liquid crystal and yet to obtain a more reasonable time response, we are attempting to put together a 10.6 μ detector by using a thin film of a cholesteric-nematic liquid crystal mixture. The method would make use of the dichroic nature of the material and the result of localized heating of the material by the laser beam would be observed by measuring the rotation of the plane of polarization of a second beam of visible radiation passing through a film. This method has been used as a sensitive temperature indicator[30] but has not, as far as we know, been used in our application.

We have done some preliminary experiments using a crude thin film placed between two polarizing plates and have observed a temperature effect. There are some techniques of surface preparation[31] which we are learning in order to make uniform films which will be tested with the laser beam.

The fundamental absorption of light in a semiconductor occurs when the energy of the photons is great enough to move electrons in the valence band to the conduction band.[32,33] It follows then that absorption occurs for

$$h\nu \geq E_c - E_v = E_g$$

where $h\nu$ is the energy of the photon, E_c is the energy of the conduction band, and E_v is the energy of the valence band. If the photon energy is less than E_g, then it will not be absorbed. Therefore, at $h\nu = E_g$ there will be an absorption edge. Since E_v depends on the electron temperature, the absorption edge will change with temperature. In 1958 Dutton[34] reported this effort for CdS. Weider[35,36] applied this to study heat flow in a film of aluminum.

We felt that if a thin film of CdS could be heated directly with a laser, the temperature rise, i.e., the change in the absorption edges, could be used to measure variations in energy output of the laser. A practical use for this would be to build a large area detector to be used to study the spatial refraction of the laser beam as it passes through a plasma when $\omega_p < \omega$ (of the incident laser beam).

The thin film was prepared by vacuum plating the CdS onto a cleaned 3-1 4-in. x 4-in. glass plate. The plate was cleaned by first washing it with

Micro Cleaning Solution and water and then rinsing with acetone. Then it was soaked in a weak aqua regia solution to leach off any surface impurities, and finally rinsed with distilled water. A small electric motor with gear assembly and rotating shaft upon which the plate was mounted was assembled in a vacuum chamber. Rotating the plate during evaporation ensured a uniform coating of the CdS. Evaporation was performed by placing a small amount of the powder in a size 00000 precelain combustion boat and heating with a filament of 20-mil tungsten wire. The thickness of the film was determined by weighing the plate before and after coating and dividing the weight of the deposited CdS by its density and the coated area of the plate. The thickness was 9500 ± 600 Å. (Note that there is question on the density of the film.[37]) Extreme care was taken to keep from touching the plate with the bare hands to avoid grease and moisture contamination of the surface. It should be noted that the toxicity of CdS is extremely high, and great care must be exercised when handling it to avoid inhalation or injection.

Figure 23 shows the detector arrangement. White light from a 30-amp 3.5 Volt General Electric Ultraviolet Spectrum Tungsten Source was apertured, sent through the CdS film and focused onto the entrace slit of a D187 Hilger and Watts glass prism monochrometer. An RCA 931A photomultiplier tube was used to monitor the light signal. The voltage divider current was 0.91 ma. This results in an anode current to voltage divider current ratio of 0.91, which is in the linear region of the P.M. tube.[38] The anode current was dropped across a resistor to ground, resulting in a voltage signal that was read on an oscilloscope connected in parallel with the resistor. Heating of the film was performed with a pulsed 1/2 joule TEA CO_2 laser. For the pulse shape see DeBoo.[39]

Variations of the absorption coefficients as a function of temperature was studied by placing the plate on an open ended metal box that was wrapped with heating tape. For this particular part of the experiment, the light source was from a Beckman D9 spectrophotometer.

The relative transmission vs. wavelength for two temperatures is plotted in Figure 24. Figure 25 shows the transmission of 5100 Å light through the film as a function of temperature. From curves like Figure 25, 5100 Å was selected as the best wavelength to be used. It should be noted that electronic noise was dominant in determining the error loss in these figures. This relatively noisy light source was the reason for changing to the F.E. Ultraviolet Spectrum Tungsten source.

When the CdS is heated by the laser, the change in transmission produces a pulse from the P.M. tube shown in the lower trace in Figure 26. The upper trace on the scope is the output from a Gen Tec Joulemeter (0.1 millijoule - 2 joule sensitivity) placed behing the laser. (The rear mirror is 98% reflecting.) This is included in order to monitor the energy output of the laser. Each division corresponds to 0.2 ± 0.05 joule. On the lower trace each division corresponds to 0.2 volt. The sweep on the scope was 0.1/msec/cm. The signal to noise is 10:1, and the rise time is 20 μsec. Table I gives information pertinent to taking the data in Figure 26.

TABLE I

EQUIPMENT INFORMATION FOR TAKING DATA IN FIGURE 26

Entrance slit	17 mm x 0.32 mm
Exit slit	20 mm x 0.18 mm
P.M. trace	0.2 V/cm
Joule Meter trace	0.1 V/cm
Oscilloscope sweep	0.1 msec/cm
Aperture	1/4-in. (D) hole placed 9 cm behind the film

The signal vanished when: (1) the laser beam was blocked, (2) the tungsten light was blocked, and (3) the entrance slit was closed. The energy density of the incident laser beam was measured to be 0.12 ± 0.05 J/cm^2. It was determined that the damage threshold of the CdS is between this value and 0.3 ± 0.1 J/cm^2.

Traces like Figure 26 show that this technique is promising for use as a laser detector for energy densities on the order of 0.12 J/cm^2 or less. The light source used presently runs on a.c. current, meaning that a high-pass filter needs to be included in the electronics between the P.M. tube and the scope to suppress the 60-cycle signal. In order to further improve the signal to noise ratio, further experimentation will include trying different combinations of aperture, entrance slit, and exit slit settings. An Argon-ion laser is also being considered as a light source since it would give a clean, intense monocrhromatic light beam.

I. DIAMOND DIE

For some time we have been using an extrusion method to produce a fine lithium wire prior to explosion. This involved extruding lithium metal through a 1 mil diameter hole in molybedenum metal. We have felt for some time that the lack of reproducibility in our experiments might be partially explained by the fact that the aperture in these dies grows rather rapidly. A search for a new extrusion die led to the use of a commercially purchased diamond die.* Although the die must be cleaned after the extrusion of about six wires, the cleaning procedure is rather simple and will allow us to make more shots per day than was possible with our present system.

*Purchased from Lithcoa, Inc.

J. RECENT X-RAY MEASUREMENTS

Theoretical studies of high Z exploding wires[40] has prompted the development of an apparatus (Figure 27) to explode several such wires (.001 in. diameter) in succession without pumping down the experimental chamber to air. The wire is attached to the brass rod or "pusher" by wrapping the wire around the hooked end and sealing the connection with glass blowing wax. The extraction operation consists of depressing the pusher while maintaining a large, variable potential (3 - 20 kV) between the wire and the lower electrode, thus the wire is pushed and pulled. The wire affixes itself upon contact with the lower electrode. Electrical contact with the upper electrode is made by surface contact in the thin channel. After firing, a combination of rotation and pushing releases the wire in the channel and the process is repeated until the wire is consumed. This operation has been successfully applied to .001 in. tungsten wire yielding eight shots per loading at 2 in. per shot. This device is currently being upgraded to use a variety of materials that have been acquired: molybdenum, iron, and aluminum.

The imaging of metallic exploding wire plasmas with soft X-rays (energies less than 5 keV) is a non-trivial task. No refractive optics exist for these X-rays, one must employ either very basic imaging techniques (e.g., pinhole camera) or diffractive techniques (e.g., coded aperture imaging—Fresnel zone plate). A further complication results from the high attenuation of these emissions by all materials including air. With these observations in mind a prototype X-ray pinhole camera was constructed (see Figure 28).

The prototype camera was open to the vacuum chamber and ambient light. The film (Kodak No-Screen) was wrapped in .001 in. aluminum foil. This protected the film from the light. Aluminum was chosen because it is readily available and inexpensive. Experiments carried out with tungsten wires demonstrated that to collect sufficient X-rays for image formation (i.e., increase pinhole size) spatial resolution was a dismal 8 mm.

As a result of the experience with the prototype camera, a new pinhole camera (Figure 29) was designed and is being constructed with several major improvements. One, the camera body may be evacuated independent of the chamber resulting in the ability to use the wire loader's multiple shot capability more fully than the prototype single shot camera. Two, the camera body is light tight: this eliminates the need to protect the film from ambient and plasma light. At the same time, this allows the use of foils that cover only the pinhole, thus fulfilling a dual function as a vacuum and light tight seal. The smaller size of foil required allows one to use more exotic and thinner foils, e.g., beryllium and nickel. The X-rays are attenuated less, thus allowing the use of a smaller pinhole and improving spatial resolution. A simple example illustrates this fact:

$x = .001$ in. Be & Al foils

$$\frac{I_{Be}}{I_{Al}} = \exp(\mu_{Al}\rho_{Al}x - \mu_{Be}\rho_{Be}x) = 17.85$$

$$I/I_o = \exp(-\mu\rho x)$$

$$\left.\begin{aligned} \mu_{Al} &= 5.5 \times 10^2 \text{ cm}^2/\text{gm} \\ \mu_{Al} &= 1.9 \times 10^2 \text{ cm}^2/\text{gm} \end{aligned}\right] \text{ Ref. 41}$$

$$\rho_{Be} = 2.702 \text{ g/cm}^3$$

$$\rho_{Be} = 1.85 \text{ g/cm}^3$$

Finally, the camera configuration is easily changed; the pinhole to film and pinhole to plasma distances may be varied independently along with the pinhole diameter, the device is adaptable to coded aperture imaging by replacing the pinhole. This renders control of resolution, magnification, and part of the plasma that is imaged to the experimenter.

Concurrent with the development of the X-ray camera, other diagnostics are being assembled. For temporal plasma temperature measurements of two foil absorber-scintillator-photomultiplier combinations have been purchased and are being assembled. Simultaneous measurements of X-ray emissions through two different foils enables one to infer the plasma temperature. This work is an extension of a pilot study done with a single detector.

Spectral information will be obtained from a recently purchased X-ray crystal (NaCl) that will be incorporated in a spectrometer.

Calibration becomes an important question, especially when one considers the crystal spectrometer and the inherent nonlinearities in No-Screen film. Two approaches have been chosen: (1) the construction of a cold cathode soft X-ray source[42], and (2) the purchase of an alpha, ^{244}cm, excited fluorescence source (Isotope Products Laboratories, Burbank, Calif.). These will be employed to calibrate diagnostics.

K. LIST OF STUDENTS AND PROJECTS PARTIALLY SUPPORTED BY GRANT

1. Thomas Blue, "Charged Particle Measurements from an Exploded Wire Plasma" (M.S. Candidate).

2. Wayne Zeuch, "Prototype Proplylene Absorption Cell—Construction and Testing" (M.S. Candidate).

3. David Brower, "Construction of a U.V. Ionized CO_2 Laser" (Undergraduate Project).

4. Monte Fowler, "CO_2 Laser Electronics" (Undergraduate Project).

5. Matt Lambert, "Wave-Guide Laser" (Undergraduate Project).

6. Albert Hanson, "Large Area CO_2 Detectors" (M.S. Project).

7. Kenjiro Takeshita, "Numerical Calculations of Exploded Wire Plasmas" (Senior Project).

8. Paul Rockett, "Pulsed Holographic Interferometry of High Density Z-Pinch and Exploded Wire Plasmas" (Ph.D. Thesis).

9. Duncan Steel, "Intense CO_2 Laser Interactions with a Dense Helium Z-Pinch Plasma" (Ph.D. Thesis).

10. John Ackenhusen, "Critical Layer Penetration in a Cold Z-Pinch Plasma By High Intensity CO_2 Laser Radiation" (Ph.D. Thesis).

L. PAPERS AND ARTICLES

I. PAPERS

1. "Application of Transmission Line Theory to Optical Resonator Analysis," D. G. Steel and P. D. Rockett. IEEE Conference on Plasma Science, Ann Arbor, Michigan, May 14-16, 1975.

2. "Ray Tracing Through a Cold, Collisionless Plasma," P. D. Rockett and J. D. DeBoo. IEEE Conference on Plasma Science, Ann Arbor, Michigan, May 14-16, 1975.

3. "Holographic Interferometric Determination of Electron Density Profiles in an Exploding Lithium Wire Plasma," P. D. Rockett. Bull. Am. Phys. Soc. 20, 1235 (1975).

*4. "Extracting Density Profiles from Z-Pinch and Exploding Wire Plasmas with Pulsed Holographic Interferometry," P. D. Rockett, D. R. Bach, and D. G. Steel. Bull. Am. Phys. Soc. 21, 1041 (1976).

5. "Penetraction of an Overdense Z-Pinch Plasma by High Intensity CO_2 Laser Light" (J. G. Ackenhusen, P. D. Rockett, D. G. Steel, and D. R. Bach). Paper presented at Seventh Annual Anomalous Absorption Conference, Ann Arbor, Michigan, May 1977.

6. "Intensity Dependent Transmission of 10.6 μ Radiation Through A Cold Overdense Z-Pinch Plasma," J. G. Ackenhusen and D. R. Bach. Bull. Am. Phys. Soc. 22, 1205 (1978).

II. ARTICLES

*1. "Absorption of CO_2 Laser Radiation in an Exploded Lithium Wire Plasma," J. C. DeBoo and D. R. Bach. J. Appl. Phys. 46, 2496 (1975).

*2. "Intensity Dependent Transmission of 10.6 Micron Radiation Through an Overdense Z-Pinch Plasma," J. G. Ackenhusen and D. R. Bach. Bull. Am. Phys. Soc. 22, 1205 (1977).

3. Paul D. Rockett, Ph.D. Thesis, "Pulsed Holographic Interferometry of High Density Z-Pinch and Exploding Wire Plasmas" (copies previously forwarded to AFOSR), 1977.

*4. "Holographic Interferometry of a High Energy Density Exploding Lithium Wire Plasma," P. D. Rockett. Accepted for publication in J. Appl. Phys., January 1979.

*5. "Interferometric Characterization of Density Dynamics of an Ultradense Z-Pinch Plasma," J. G. Ackenhusen and D. R. Bach. Accepted for publication in J. Appl. Phys., 1979.

*6. "Laser Driven Hydrodynamic Perturbation in an Overdense Z-Pinch Plasma," J. G. Ackenhusen and D. R. Bach. Accepted for publication in J. Appl. Phys., 1979.

Note: Papers and articles marked by (*) were partially supported by the National Science Foundation and The University of Michigan as well as the U.S. Air Force Office of Scientific Research.

REFERENCES

1. Exploding Wires, Vol. 4, W. G. Chase and H. K. Moore, eds., Plenum Press, New York, 1968.

2. D. Mosher, S. J. Stephanakis, I. M. Vitkovitsky, C. M. Dozier, L. S. Levine, and D. J. Nagel, Appl. Phys. Letters 23, 429 (1973).

3. J. C. DeBoo and D. R. Bach, J. Appl. Phys. 46, 2496 (1975).

4. P. D. Rockett and J. C. DeBoo, IEEE Conf. Rec., 2nd Int'l. Conf. on Plasma Science, 120, May 14-16, 1975.

5. D. T. Attwood, L. W. Coleman, and D. W. Sweeny, Appl. Phys. Letters 26, 616 (1975).

6. R. J. Radley, Jr., Phys. Fluids 18, 175 (1975).

7. J. G. Kelly and L. P Mix, J. Appl. Phys. 46, 1084 (1975).

8. R. A. Alpher and D. R. White, Phys. Fluids 2, 162 (1959).

9. A. J. Alcock and S. A. Ramsden, Appl. Phys. Letters 8, 187 (1966)

10. R. A. Jeffries, Phys. Fluids 13, 210 (1970).

11. J. A. Seftor, J. Appl. Phys. 45, 2903 (1974).

12. J. L. Seftor, J. Appl. Phys. 44, 4965 (1973).

13. L. D. Siebert, Appl. Opt. 10, 632 (1971).

14. D. G. Steel, private communication.

15. E. Oktay and D. R. Bach, J. Appl. Phys. 41, 1716 (1970).

16. Born and Wolf, Principles of Optics, 5th ed., Pergamon Press, New York, 1975.

17. Hirschfelder, Curtiss, and Bird, Molecular Theory of Gases and Liquids, J. Wiley and Sons, New York, 1954.

18. W. Wiese, M. Smith, and, B. Glennon, Atomic Transition Probabilities, 1, Hydrogen Through Neon, NRSDS-NBS 4 (1966).

19. J. Watts, "Theory of Multiple Resonant Reflectors," Appl. Optics 7, 1621-1623 (August 1968).

20. H. Mahlein and G. Schollmeier, "Analysis and Synthesis of Periodic Optical Resonant Reflectors," Appl. Optics 8, 1197-1202 (June 1969).

21. Procik Wiggens and Pliva, "Optical Tolerances and Electric Fields in Resonant Reflectors," Appl. Optics 10, 304-310 (February 19719.

22. M. Hercher, "Single-Mode Operation of a Q-Switched Ruby Laser," Appl. Phys. Letters 7, 39-41 (July 15, 1965).

23. W. R. Sooy, "The Natural Selection of Modes in a Passive Q-Switched Laser," Appl. Phys. Letters 7, 36-37 (July 15, 1965).

24. Drawin and Felenbok, Data for Plasmas in Local Thermodynamic Equilibrium (Gauthier-Villas, Paris, 1965).

25. F. C. Jahoda et al., Phys. Rev. 119, 843 (1960).

26. A. J. Meyerott, P. C. Fisher, and D. T. Roethig, Rev. Sci. Inst. 35, 669 (1964).

27. D. Duston, Ph.D. Thesis (The University of Michigan), 1977.

28. C. W. Smith, Appl. Phys. Letters 24, 453 (1974).

29. Linda T. Creagh and Allen R. Kmetz, *Molecular Crystals and Liquid Crystals* 24, 59 (1973 .

30. C. W. Smith, Appl. Phys. Letters 24, 453 (1974).

31. Linda T. Creagh and Allen R. Kmetz, Molecular Crystals and Liquid Crystals 24, 59 (1973).

32. K. Seeger, Semiconductor Physics, Springer-Verlag Wein, New York (1973).

33. R. A. Smith, Semiconductors, Cambridge University Press, Cambridge (1961).

34. D. Dutton, Phys. Rev. 112, 3, 785 (1958).

35. H. Wieder, J. Appl. Phys. 43, 7, 3213 (1972).

36. H. Wieder, Laser Focus, 86, May 1975.

37. J. Gottesman and W.G C. Ferguson, J. Opt. Soc. Am. 44, 5, 368 (1954).

38. R.C.A. Photomultiplier Handbook Technical Series PT-61, p. 103, 1970.

39. J. C. DeBoo, Laser Absorption in a Dense Lithium Plasma, Ph.D. Dissertation, Department of Nuclear Engineering, The University of Michigan, 1973.

40. D. Duston, Ph.D. Thesis (The University of Michigan), 1977.

41. B. L. Henke, and M. L. Schattenburg, Advances in X-ray Analysis, Vol. 18, Plenum Press, New York, 1975.

42. J. S. Solom, and W. L. Baun, Review of Scientific Instruments, Vol. 40, 1458.

FIGURES

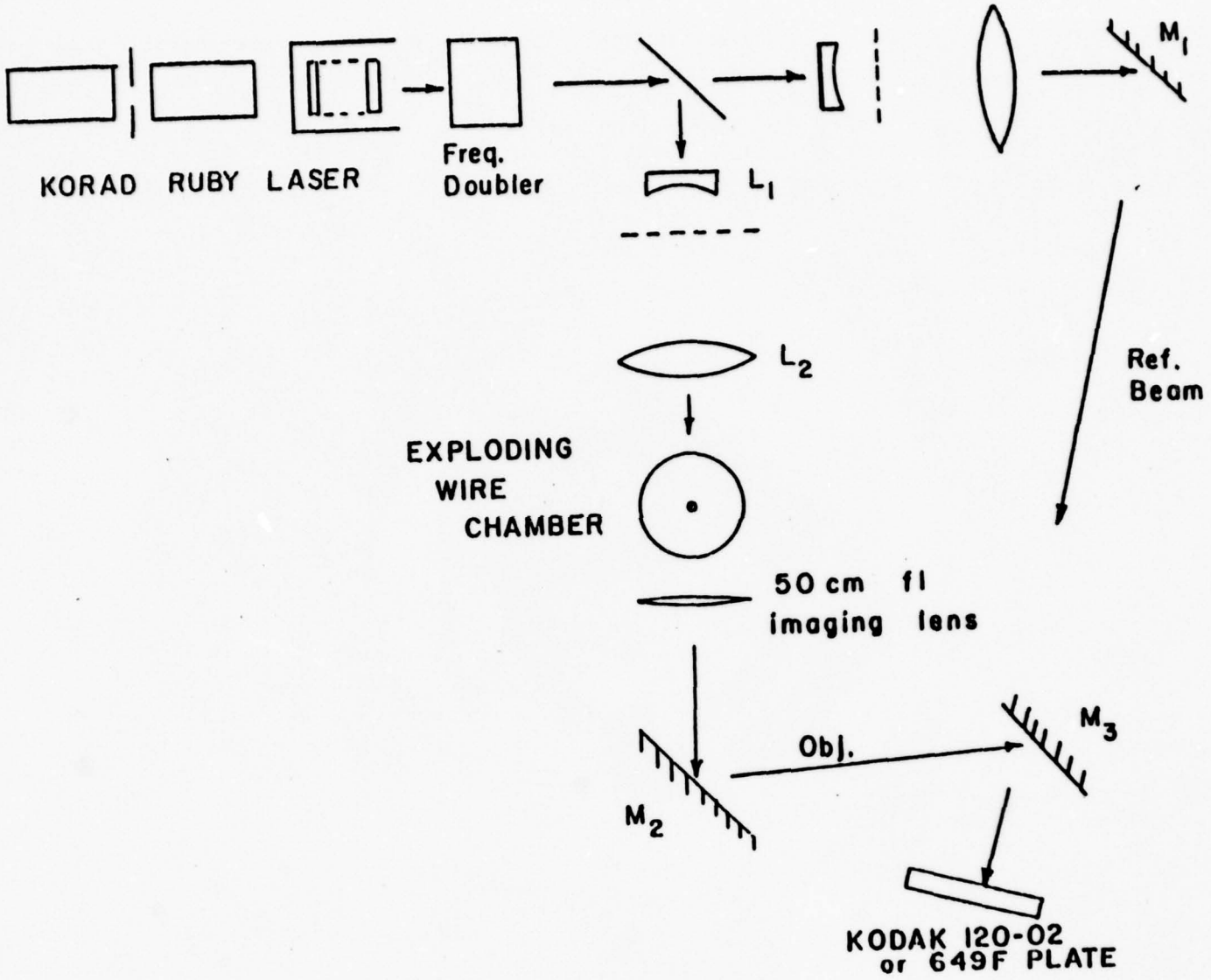
KORAD RUBY LASER
Freq. Doubler
L_1
M_1
Ref. Beam
L_2
EXPLODING WIRE CHAMBER
50 cm fl imaging lens
M_3
Obj.
M_2
KODAK 120-02 or 649F PLATE

Figure 1

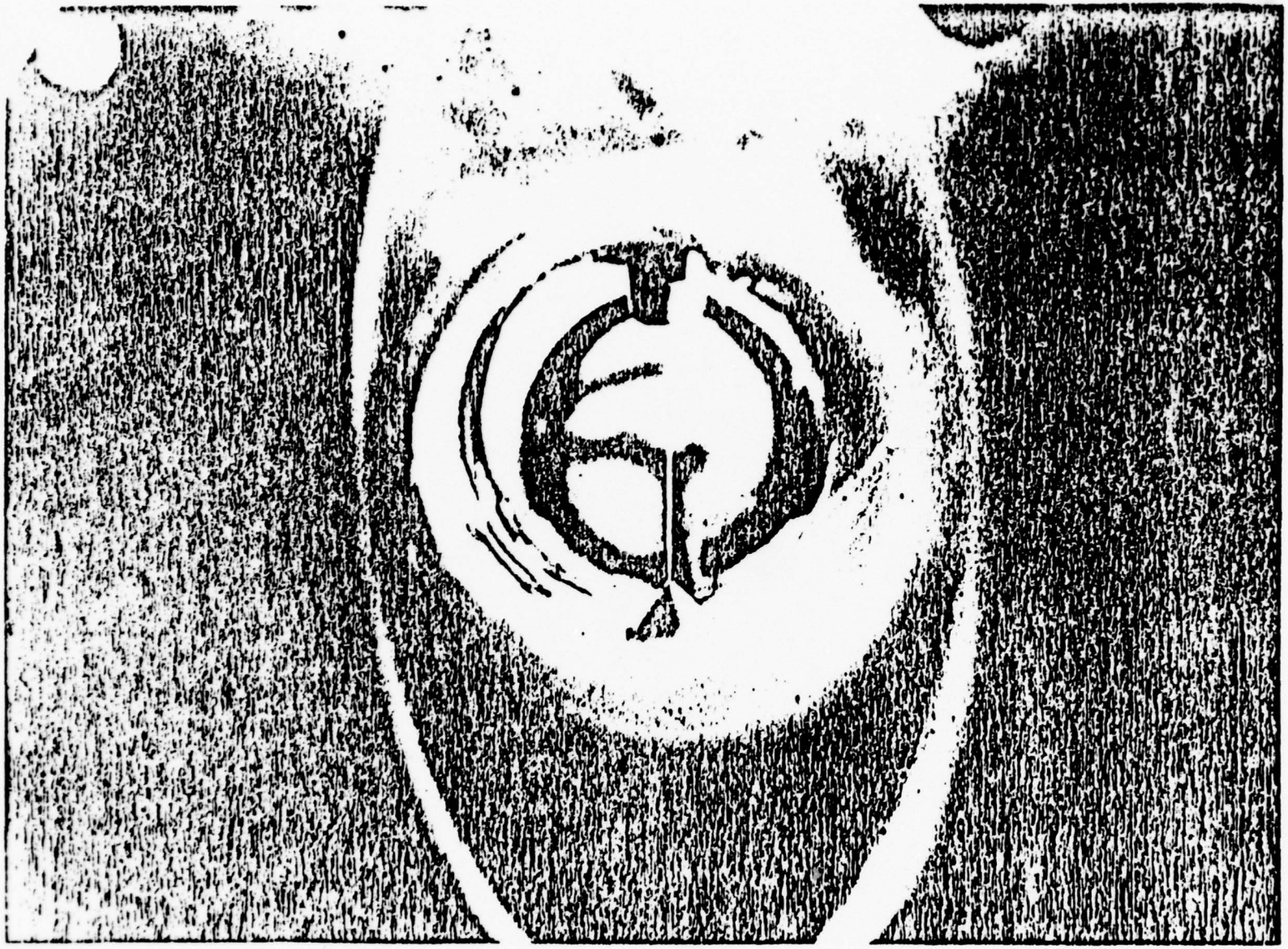

Figure 2

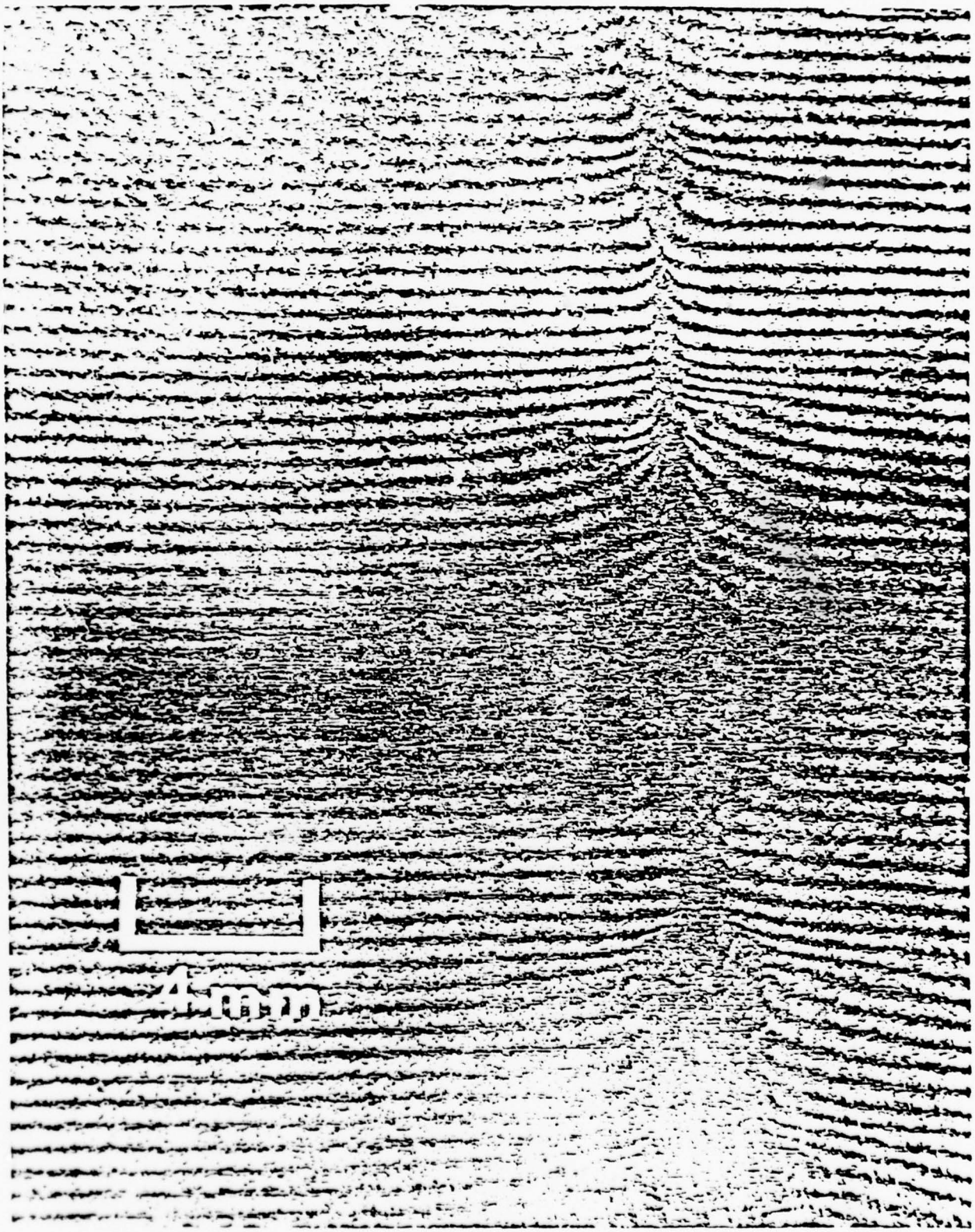

Figure 3

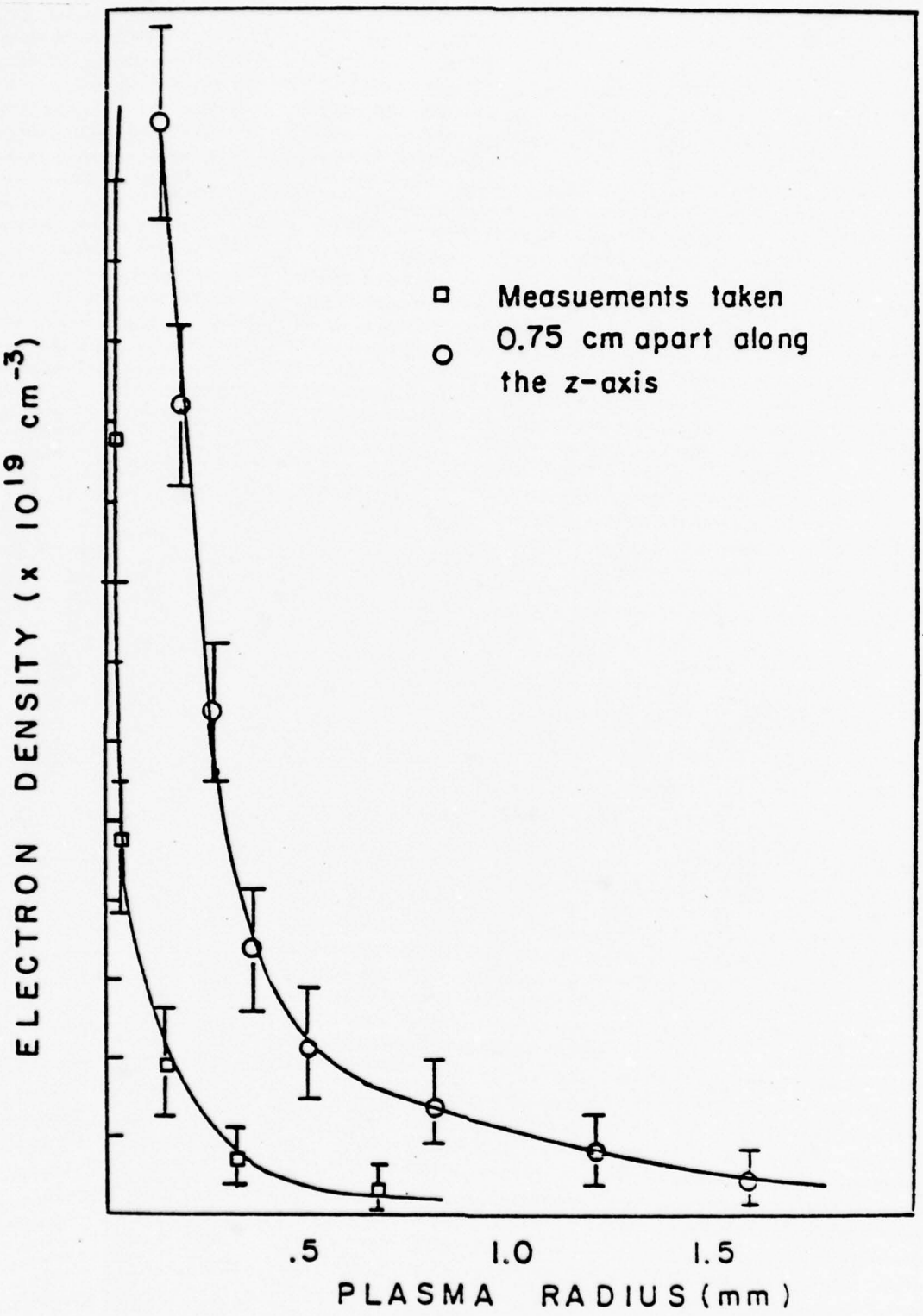
Measuements taken
0.75 cm apart along
the z-axis
ELECTRON DENSITY (x 10^19 cm^-3)
.5
1.0
1.5
PLASMA RADIUS (mm)

Figure 4

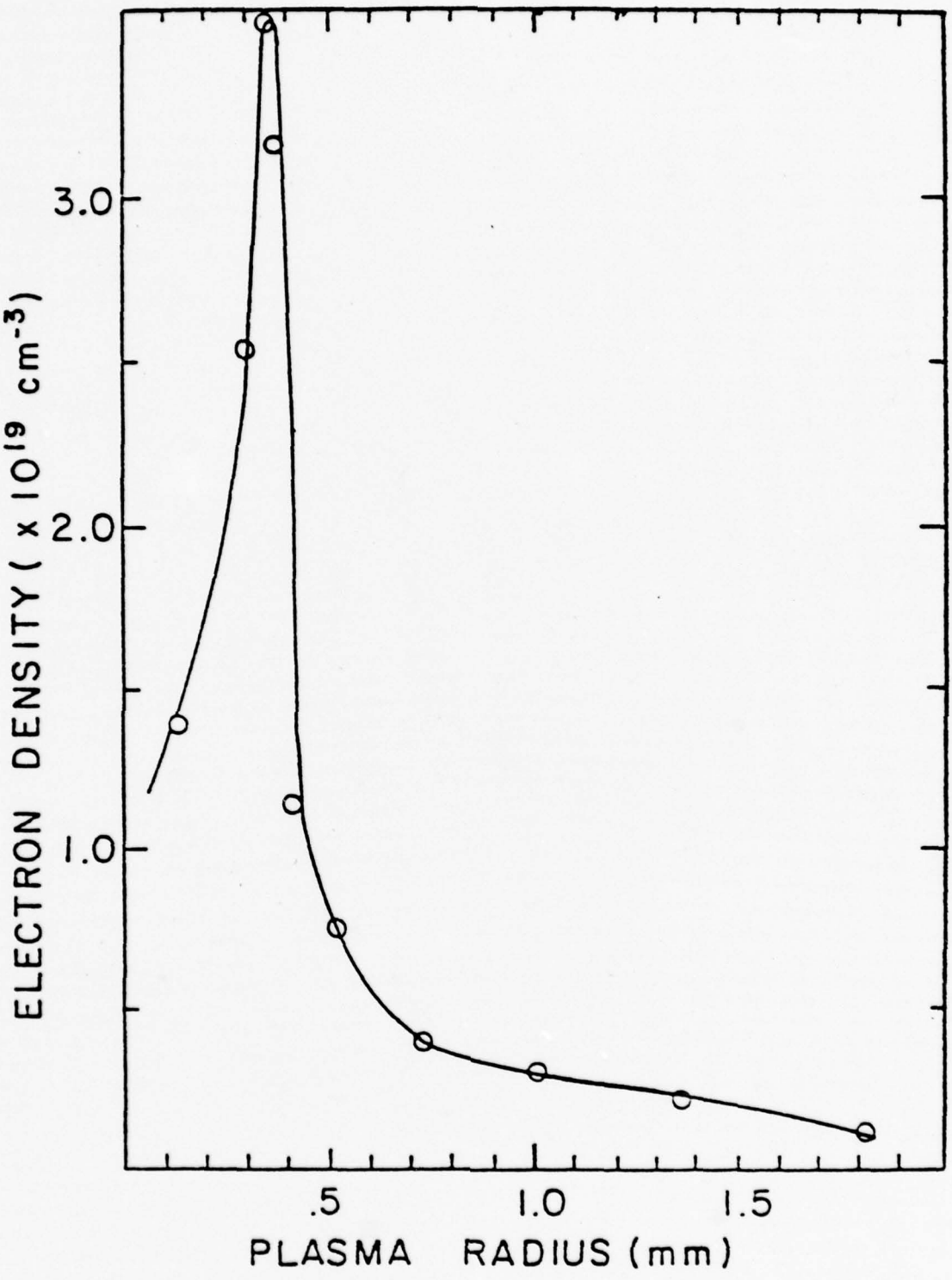

Figure 5

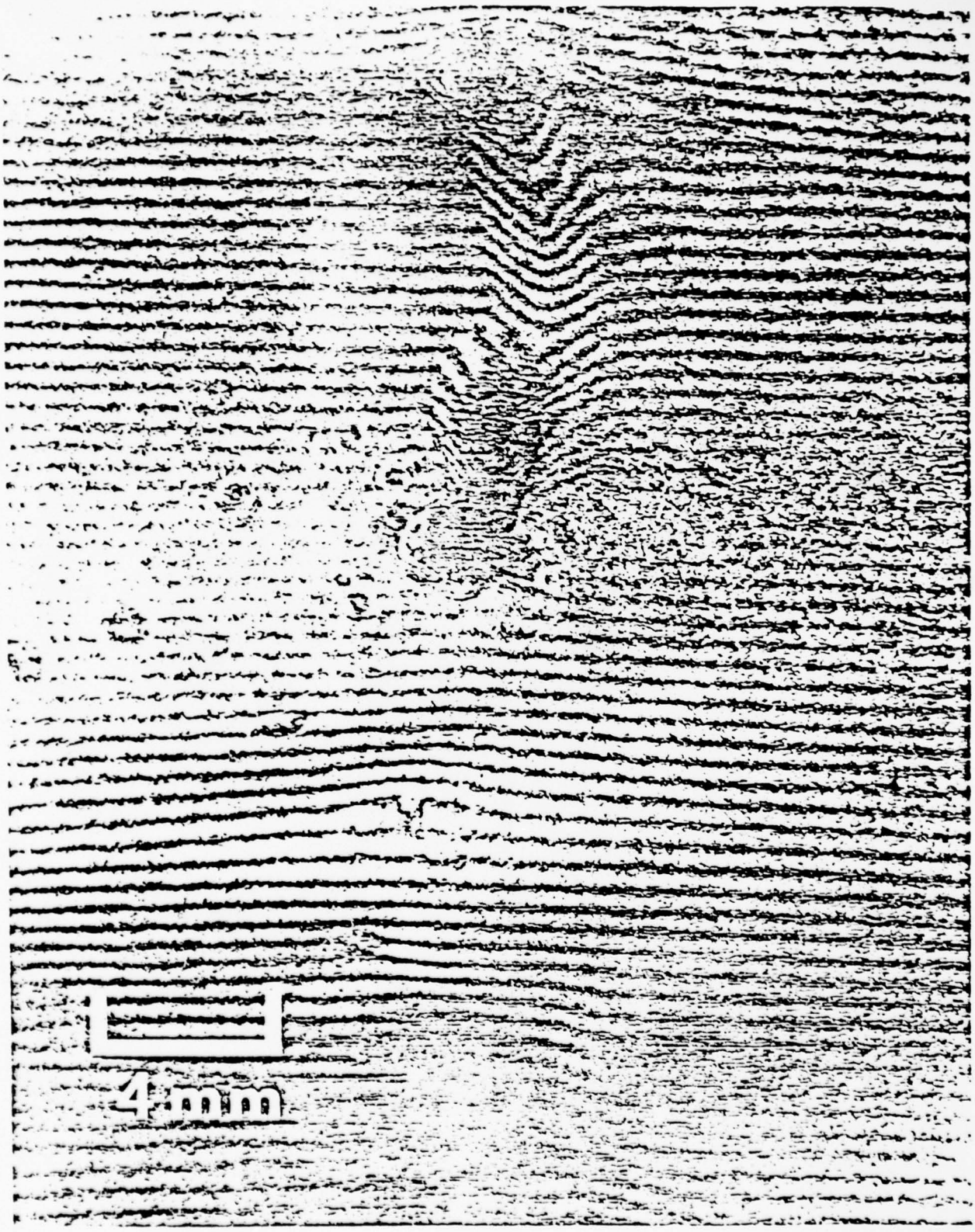

Figure 6

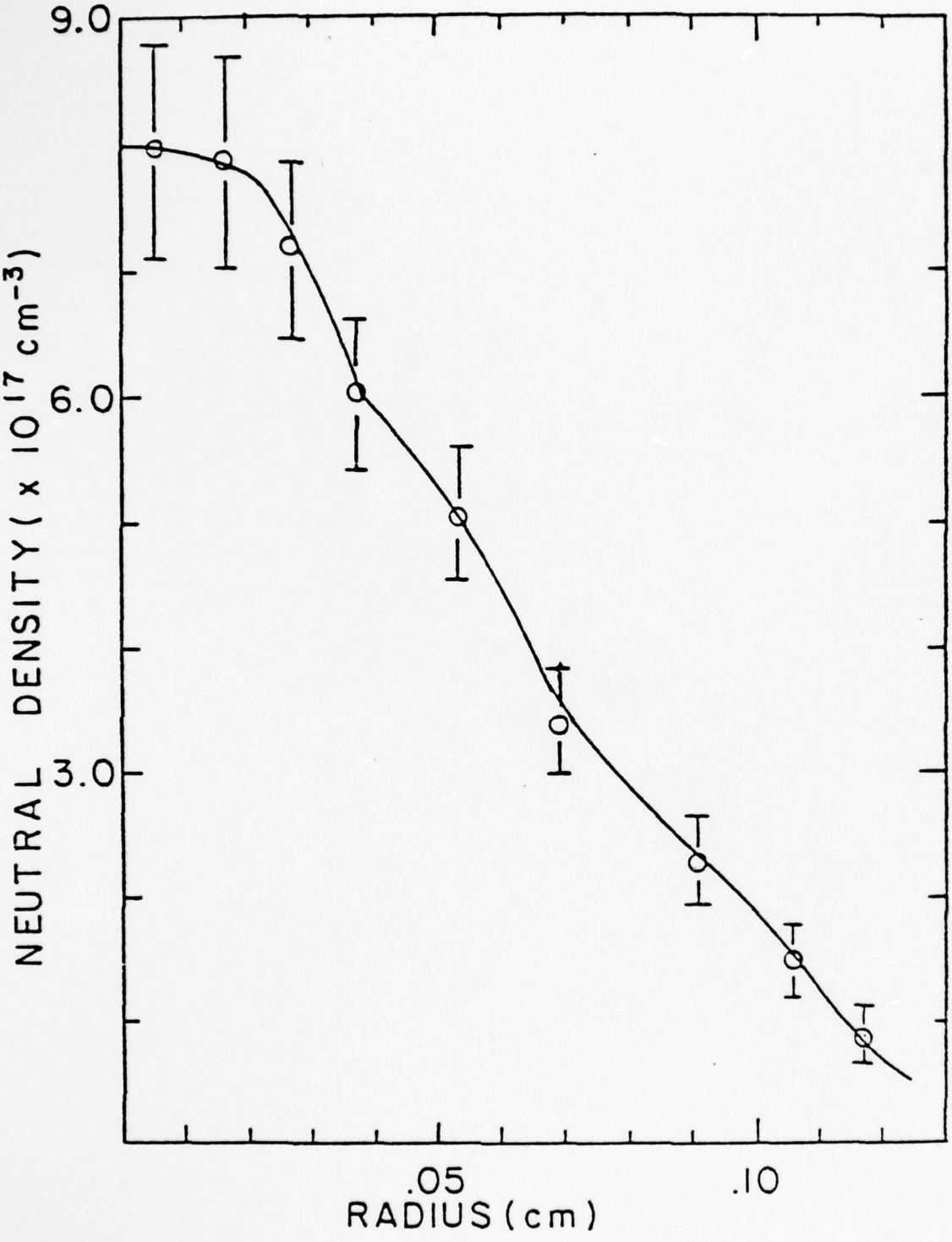

Figure 7

BOUGUER'S FORMULA

$$N(r) \cdot r \cdot \sin\phi = \text{CONST.}$$

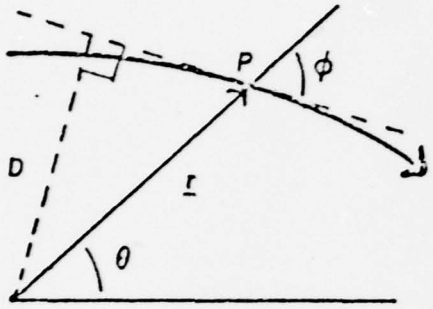

N = INDEX OF REFRACTION

ϕ = ANGLE BETWEEN $\underline{r}$ AND TANGENT TO RAY AT P

note: $r \cdot \sin\phi = D$

Figure 8

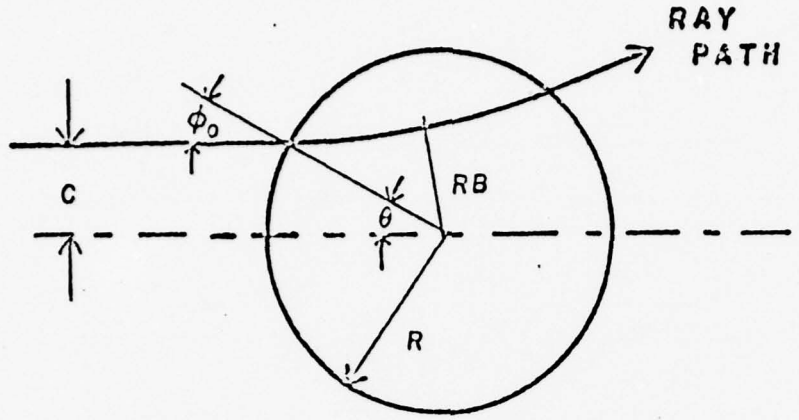

C = IMPACT PARAMETER

RB = DISTANCE OF
CLOSEST APPROACH

$$N(R) \cdot R \cdot \sin \phi_0 = C$$

$$N(RB) \cdot RB = C \quad , \quad (\phi = 90^\circ)$$

$$\therefore \quad RB = \frac{C}{N(RB)}$$

Figure 9

$$\sin\phi = \frac{r(\theta)}{\sqrt{r^2(\theta) + \left(\frac{dr}{d\theta}\right)^2}} \qquad \ldots\ldots (1)$$

USING $N \cdot r \cdot \sin\phi = C$ YIELDS $\quad d\theta = \frac{C}{r} \frac{dr}{\sqrt{N^2 r^2 - C^2}} \quad \ldots (2)$

$$\therefore \quad \boxed{\Delta\theta(R \rightarrow RB) = \int_{RB}^{R} \frac{C}{r} \frac{dr}{\sqrt{N^2 r^2 - C^2}}} \qquad \ldots (3)$$

INTEGRATE BY PARTS!

Figure 10

TO RAISE SINGULARITY OUT OF DENOMINATOR

$$\Delta\theta(R \rightarrow RB) = \frac{C}{R} \int_{\frac{RB}{R}}^{1.0} 2 \cdot \frac{1}{2} \frac{dX}{X\sqrt{NX - B}\ \sqrt{NX + B}} \cdot \frac{(N + XN')}{(N + XN')}$$

WHERE

$$U = \frac{2}{X\sqrt{NX + B}\ (N + XN')} \qquad V = \sqrt{NX - B}$$

$$N' = \frac{dN}{dX} \qquad dV = \frac{1}{2} \frac{N + XN'}{\sqrt{NX - B}} dX$$

Figure 11

YIELDS

$$\frac{R}{C}\Delta\theta(R \rightarrow RB) = \frac{2\,(N(1) - B)^{1/2}}{(N(1) + N'(1))\cdot(N(1) + B)^{1/2}} + \int_{\frac{RB}{R}}^{1.0} (NX - B)^{1/2}\left(\frac{dU}{dX}\right)dX \quad \ldots(4)$$

WHERE $X = \frac{r}{R}$, $B = \frac{C}{R}$, AND $\frac{dU}{dX} = F'N.(N, N', N'')$

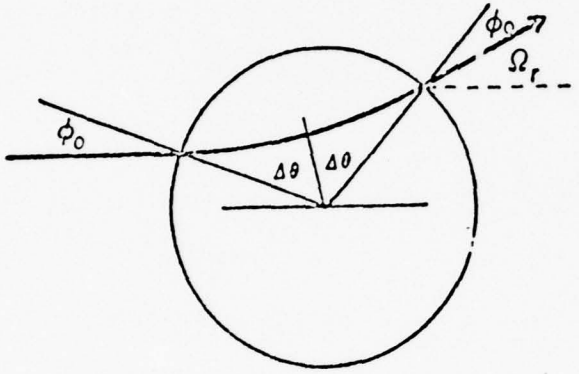

ANGLE OF REFRACTION

$$\Omega_r = 180^o - 2(\Delta\theta + \phi_o)$$

Figure 12

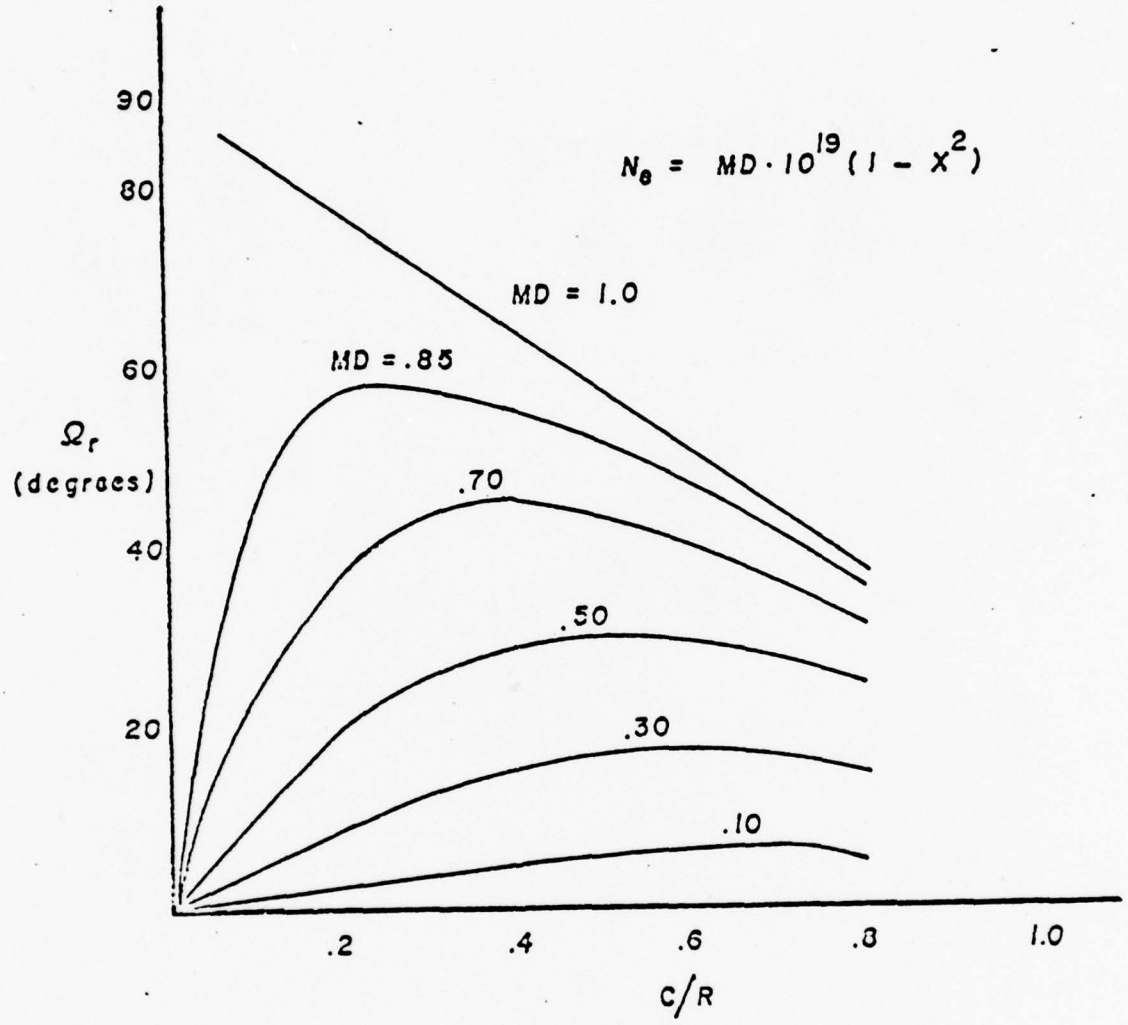
$N_e = MD \cdot 10^{19}(1 - X^2)$
MD = 1.0
MD = .85
.70
.50
.30
.10
90
80
60
40
20
Ω_r
(degrees)
.2
.4
.6
.8
1.0
C/R

Figure 13

TRANSMISSION LINE EQUATIONS

$$V = V_+ e^{-j\beta Z} + V_- e^{j\beta Z}$$

$$I = \frac{1}{Z_o}\left[V_+ e^{-j\beta Z} - V_- e^{j\beta Z}\right]$$

$$\beta = \omega\sqrt{LC}$$

$$Z_o = \sqrt{\frac{L}{C}}$$

PLANE WAVE THEORY & MAXWELL'S EQNS.

$$E_X(Z) = E_+ e^{-jKZ} + E_- e^{jKZ}$$

$$H_Y(Z) = \frac{1}{\eta}\left[E_+ e^{-jKZ} - E_- e^{jKZ}\right]$$

$$K = \omega\sqrt{\mu\epsilon}$$

$$\eta = \sqrt{\frac{\mu}{\epsilon}}$$

Figure 14

IMPEDANCE : $Z = \frac{V}{I}$

$Z = \frac{E_X(Z)}{H_Y(Z)} = \eta$; AWAY FROM INTERFACES

REFLECTION COEFF.: $\Gamma = \frac{Z_L - Z_o}{Z_L + Z_o}$

$\Gamma = \frac{\eta_2 - \eta_1}{\eta_2 + \eta_1} = \frac{E_-}{E_+}$

$Z_{IN} = Z_o \frac{Z_L + Z_o \, TAN \beta L}{Z_o + Z_L \, TAN \beta L}$

$Z_{IN_1} = \eta_1 \frac{\eta_2 + \eta_1 \, TAN \, KL_1}{\eta_2 + \eta_1 \, TAN \, KL_1}$

$K = \omega \sqrt{\mu_1 \epsilon_1}$ $\quad L_1 = N_1 z_1$

$\eta_{1,2} = \sqrt{\frac{\mu_o}{\epsilon_{1,2}}}$

Figure 15

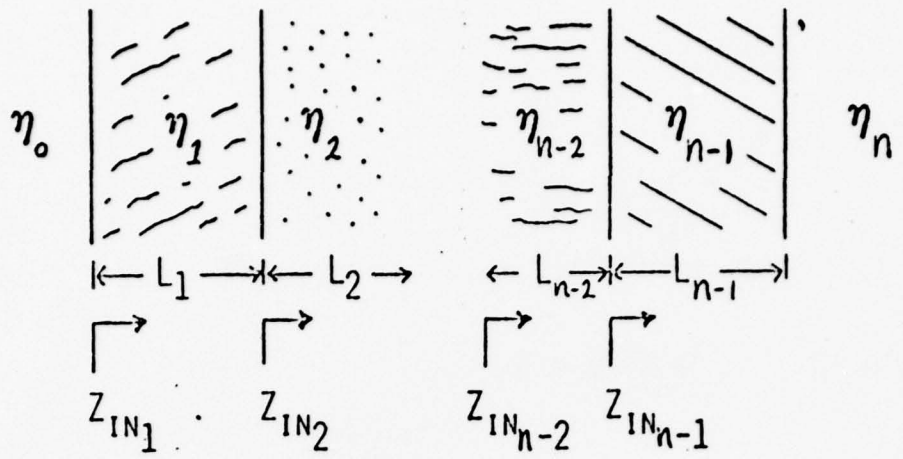

$$Z_{IN_{n-1}} = \eta_{n-1} \frac{\eta_n + \eta_{n-1}\, j\,\text{TAN}\, K_{n-1}L_{n-1}}{\eta_{n-1} + \eta_n\, j\,\text{TAN}\, K_{n-1}L_{n-1}}$$

$$\vdots \qquad\qquad \vdots$$

$$Z_{IN_1} = \eta_1 \frac{Z_{IN_2} + \eta_1\, j\,\text{TAN}\, K_1L_1}{\eta_1 + Z_{IN_2}\, j\,\text{TAN}\, K_1L_1}$$

THUS

$$\Gamma_{TOTAL} = \frac{Z_{IN_1} - \eta_o}{Z_{IN_1} + \eta_o}$$

Figure 16

GAIN DIFFERENTIATION BETWEEN MODES M & N

$$\frac{P_N(T)}{P_M(T)} = \left[\frac{R_N}{R_M}\right]^Q$$

P_N = POWER IN N^{TH} MODE

R_N = REFLECTIVITY

Q = NUMBER OF LOOP TRANSITS

TYPICAL GIANT PULSE BUILD-UP TIMES:

ACTIVE Q-SWITCH, $Q \approx 35$

PASSIVE Q SWITCH, $Q \approx 700$

Figure 17

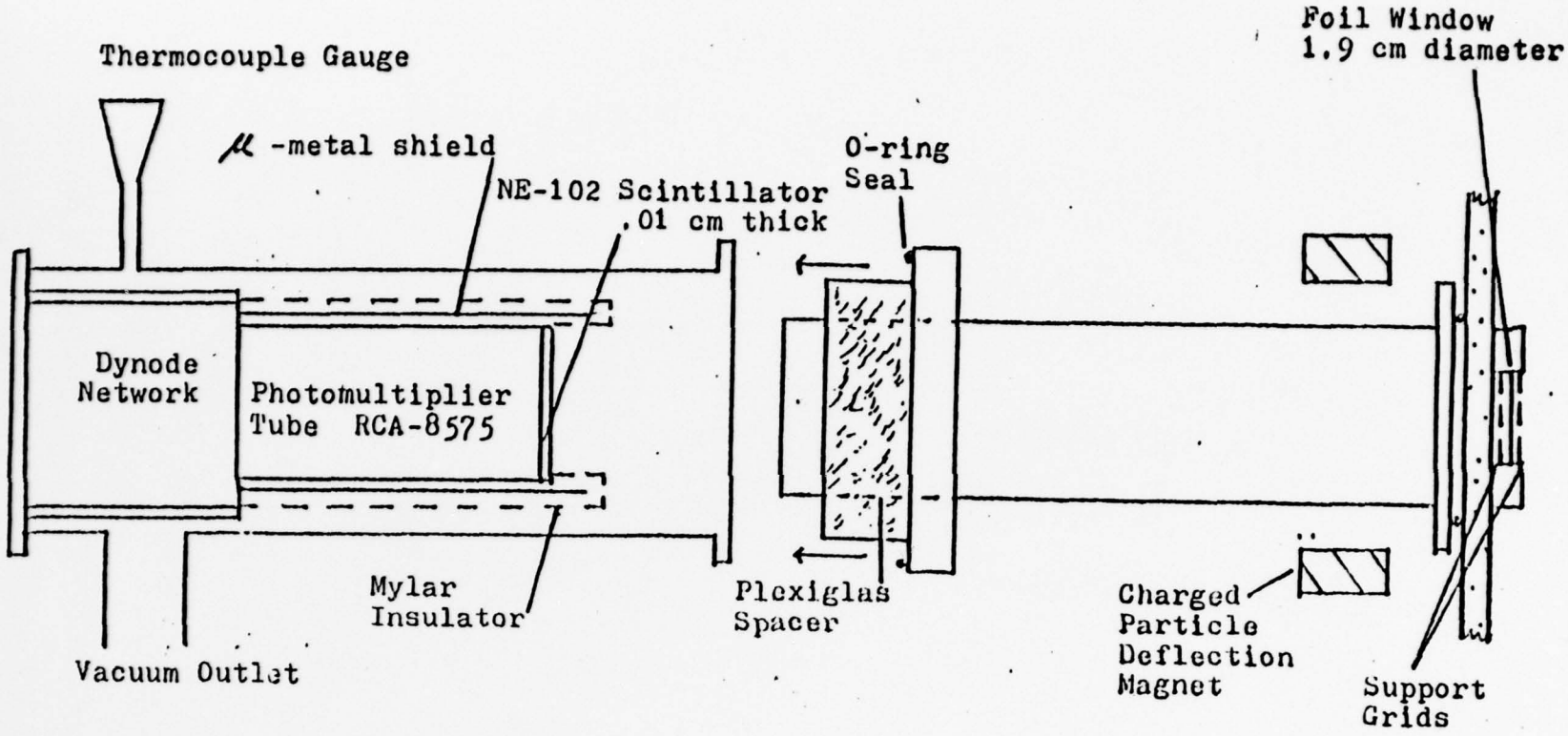

Figure 18. X-Ray Detector Used on Exploding Wire Plasma.

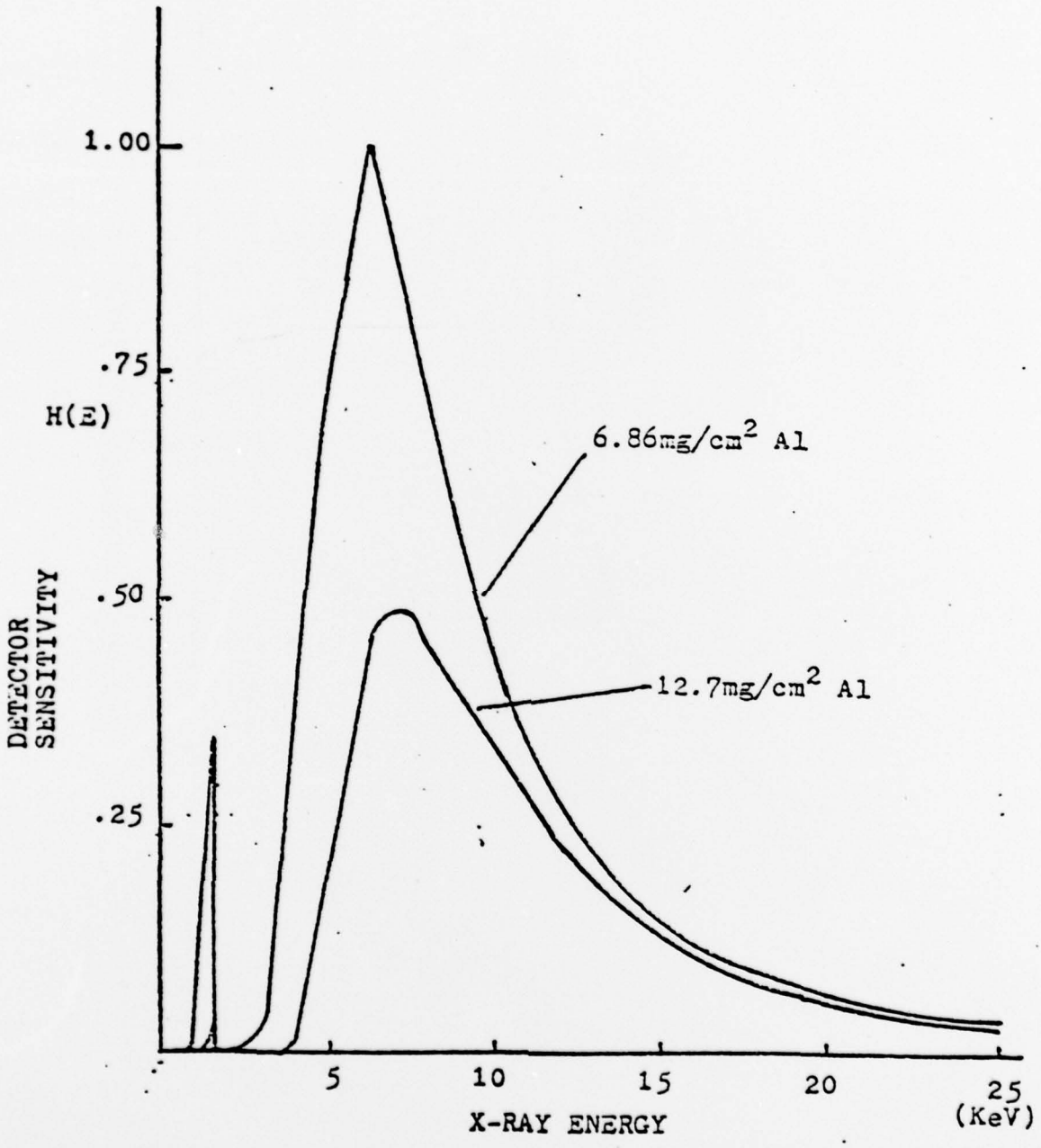
1.00
.75
.50
.25
H(E)
DETECTOR SENSITIVITY
6.86mg/cm² Al
12.7mg/cm² Al
5
10
15
20
25
(KeV)
X-RAY ENERGY

Figure 19

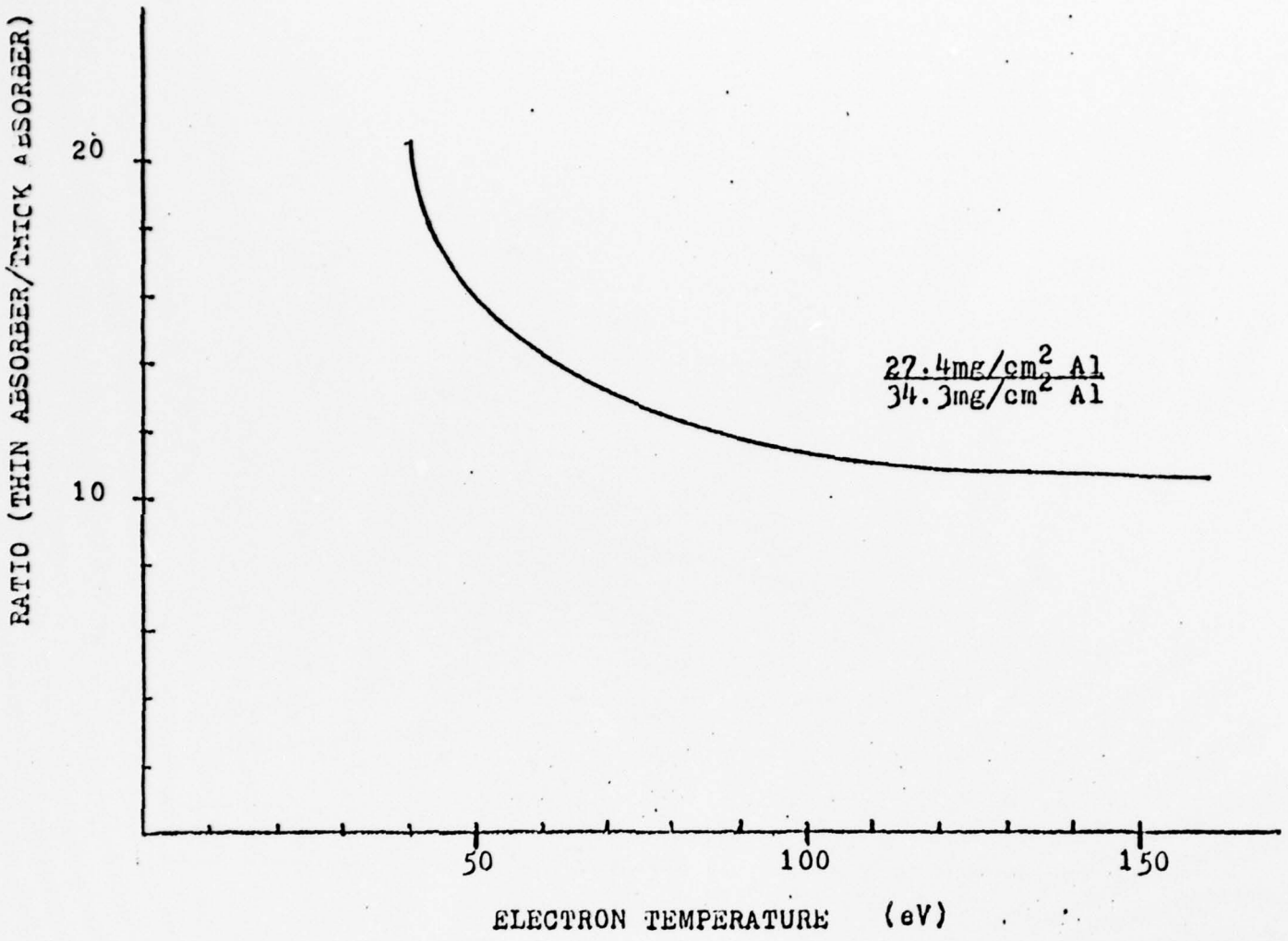
RATIO (THIN ABSORBER/THICK ABSORBER)
20
10
27.4mg/cm² Al
34.3mg/cm² Al
50
100
150
ELECTRON TEMPERATURE (eV)

Figure 20

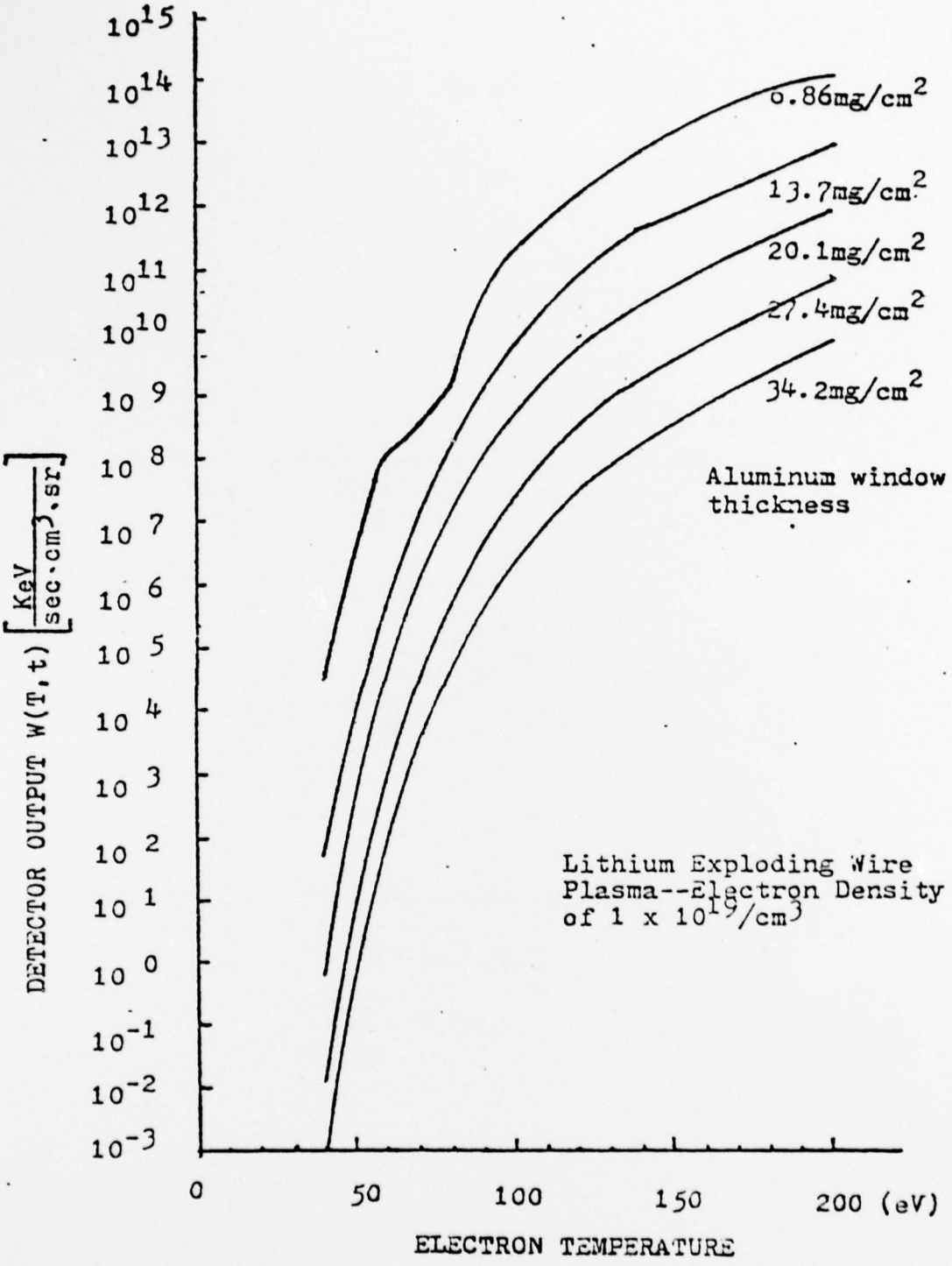
DETECTOR OUTPUT W(T,t) [KeV / sec·cm³·sr]
10^15
10^14
10^13
10^12
10^11
10^10
10^9
10^8
10^7
10^6
10^5
10^4
10^3
10^2
10^1
10^0
10^-1
10^-2
10^-3
0.86mg/cm²
13.7mg/cm²
20.1mg/cm²
27.4mg/cm²
34.2mg/cm²
Aluminum window thickness
Lithium Exploding Wire Plasma--Electron Density of 1 x 10^19/cm³
0
50
100
150
200 (eV)
ELECTRON TEMPERATURE

Figure 21

X-RAY SIGNAL AND $\frac{dI}{dt}$ vs. TIME

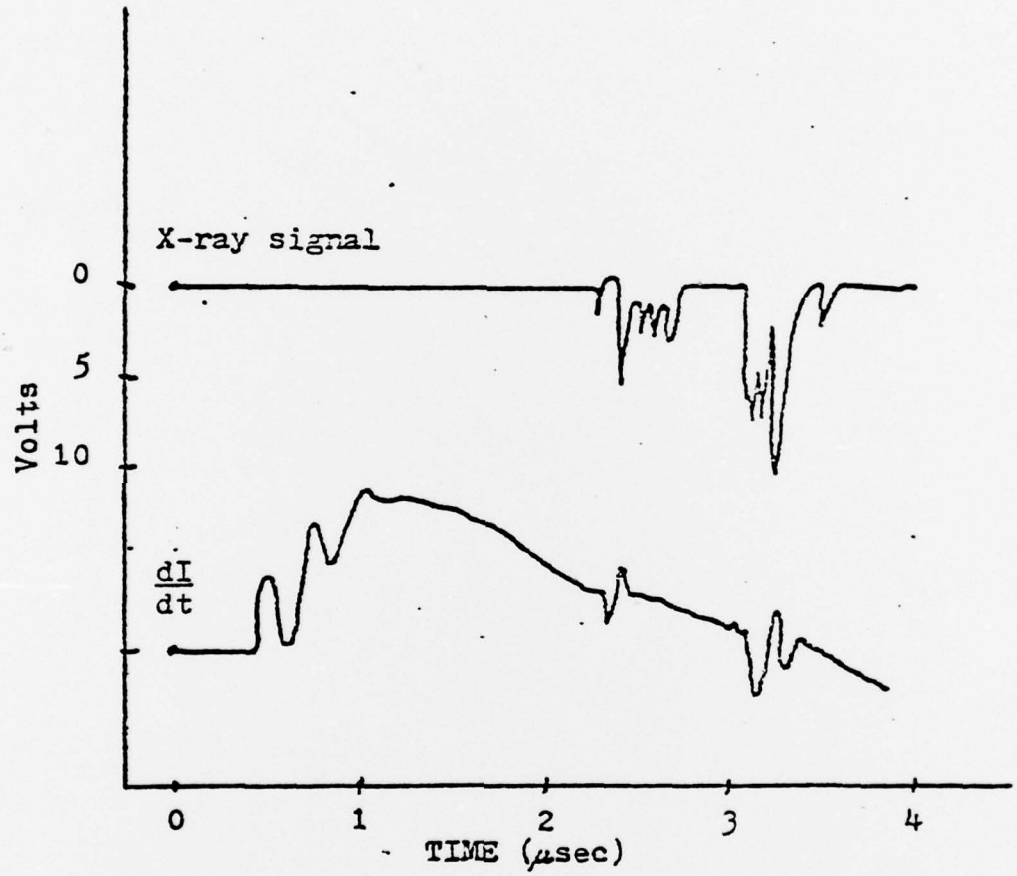

Figure 22

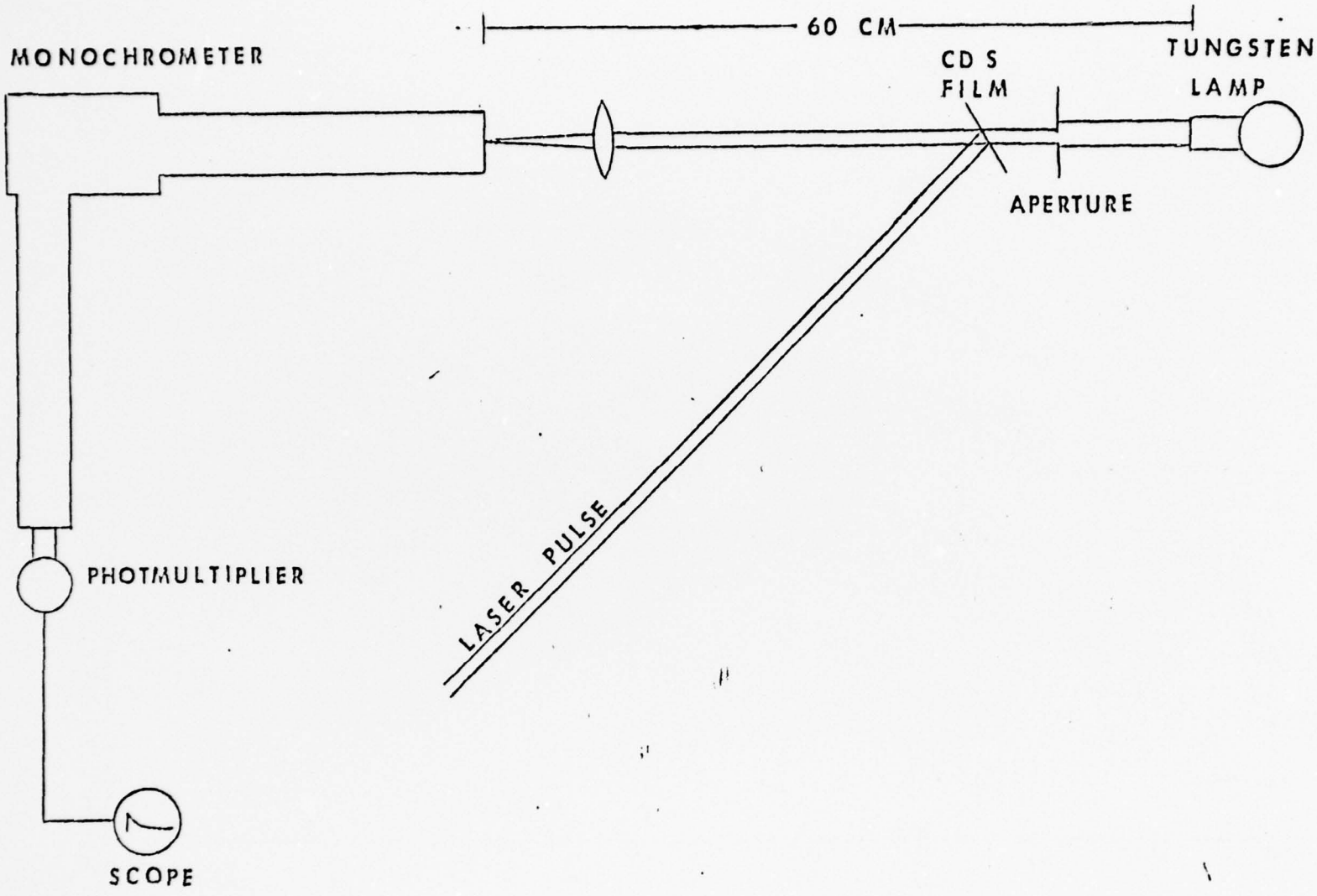
60 CM
MONOCHROMETER
CD S
FILM
TUNGSTEN
LAMP
APERTURE
LASER PULSE
PHOTMULTIPLIER
SCOPE

Figure 23

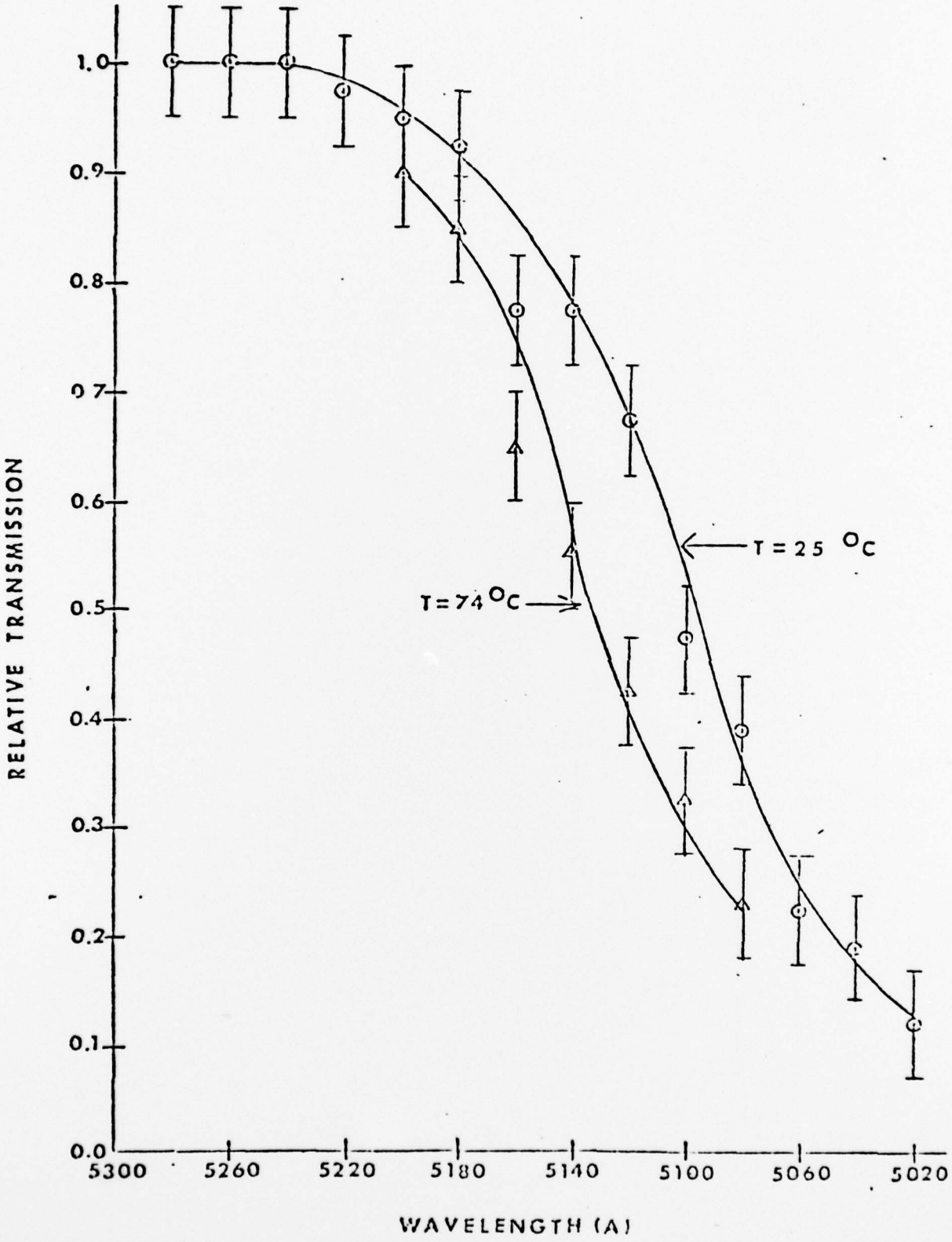

Figure 24. Relative Transmission of Light Through CdS.

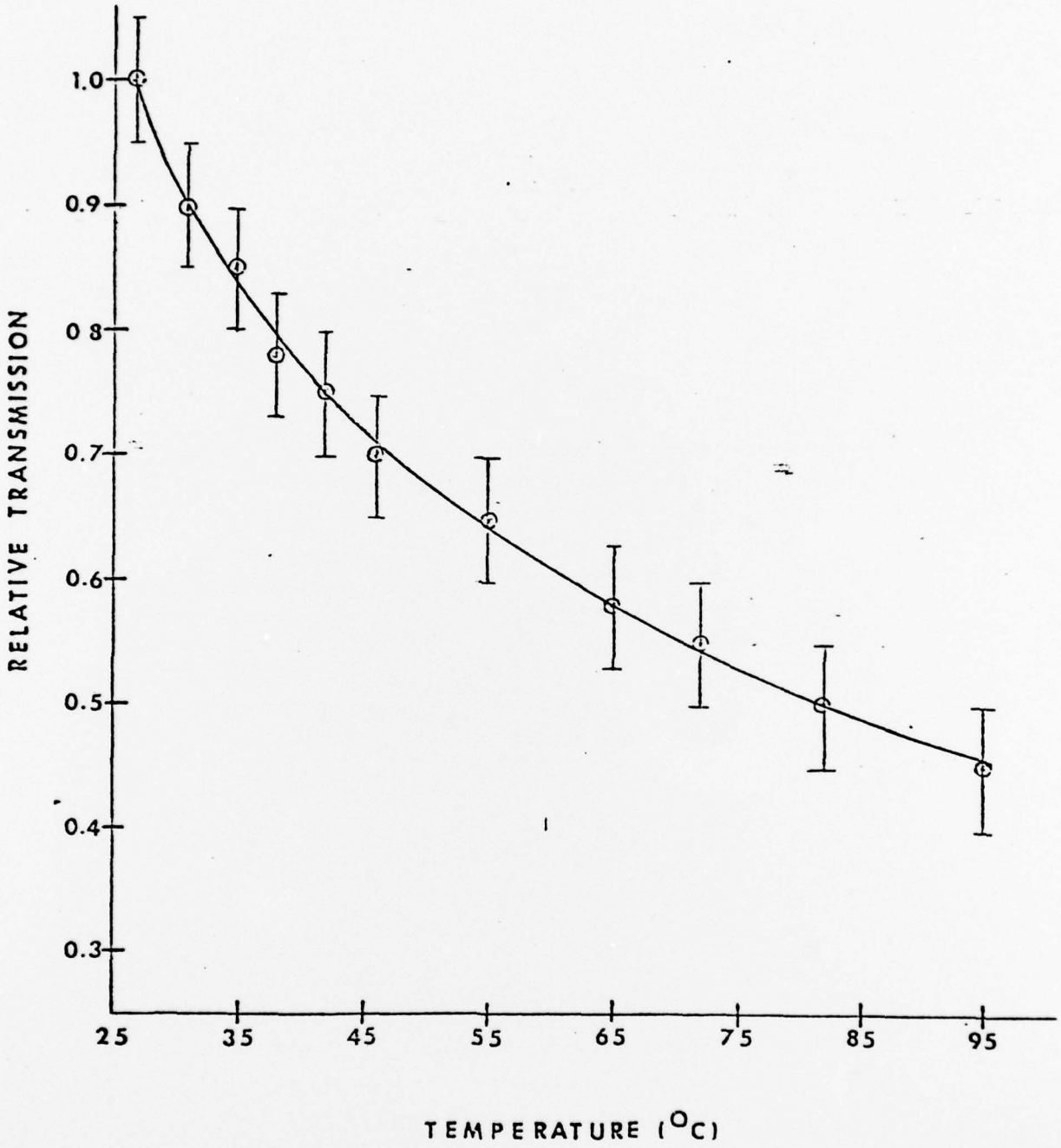

Figure 25. Relative Transmission of 5100 Å Light Through CdS as a Function of Temperature.

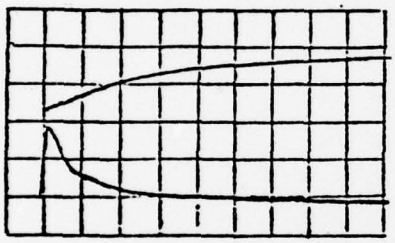

Figure 26. Photomultiplier Tube and Joulemeter Responses. Time scale: 0.1 msec/cm.

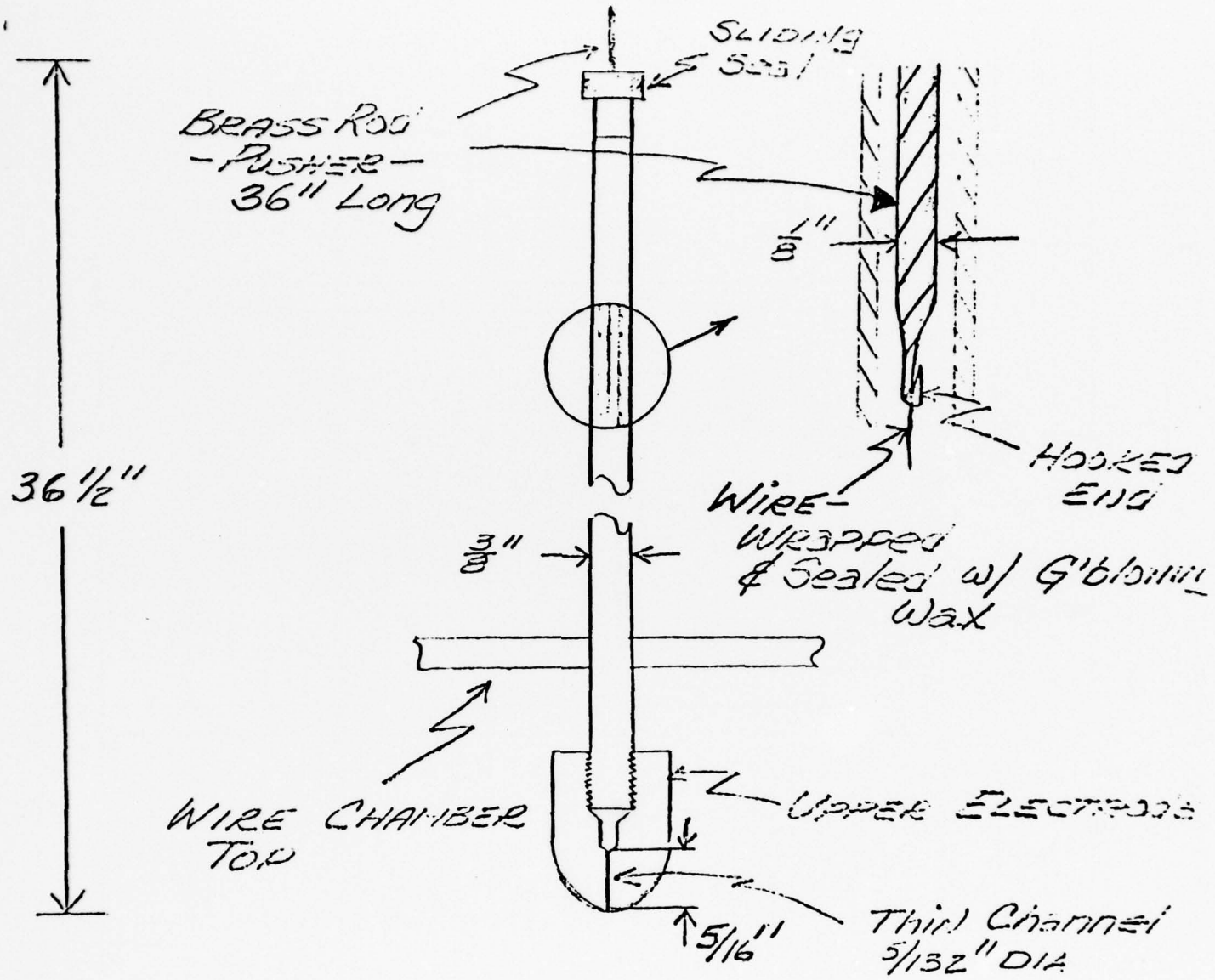

Figure 27. Solid Wire Extracting Device for Exploding Wire.

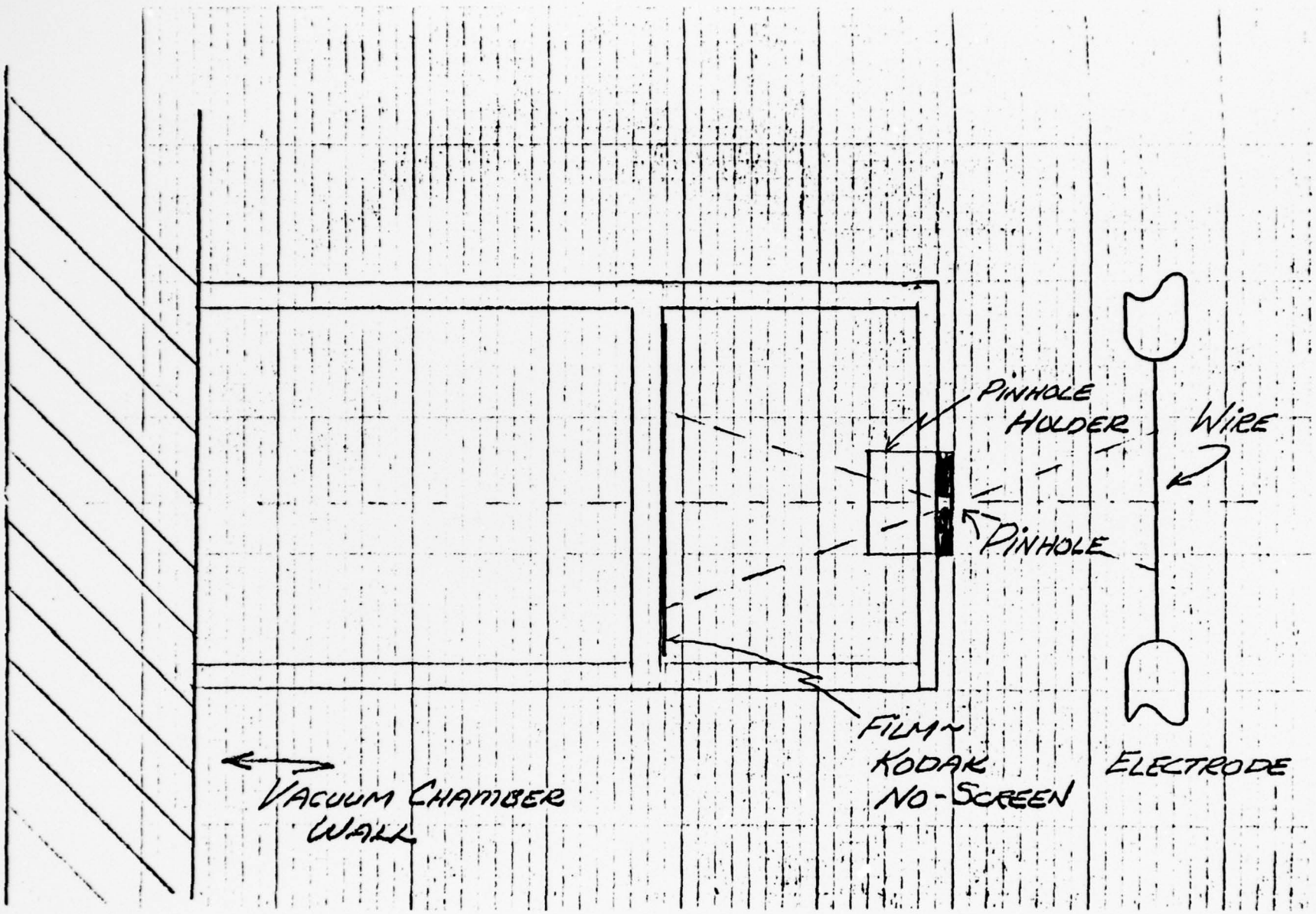

Figure 28. Prototype Pinhole Camera.

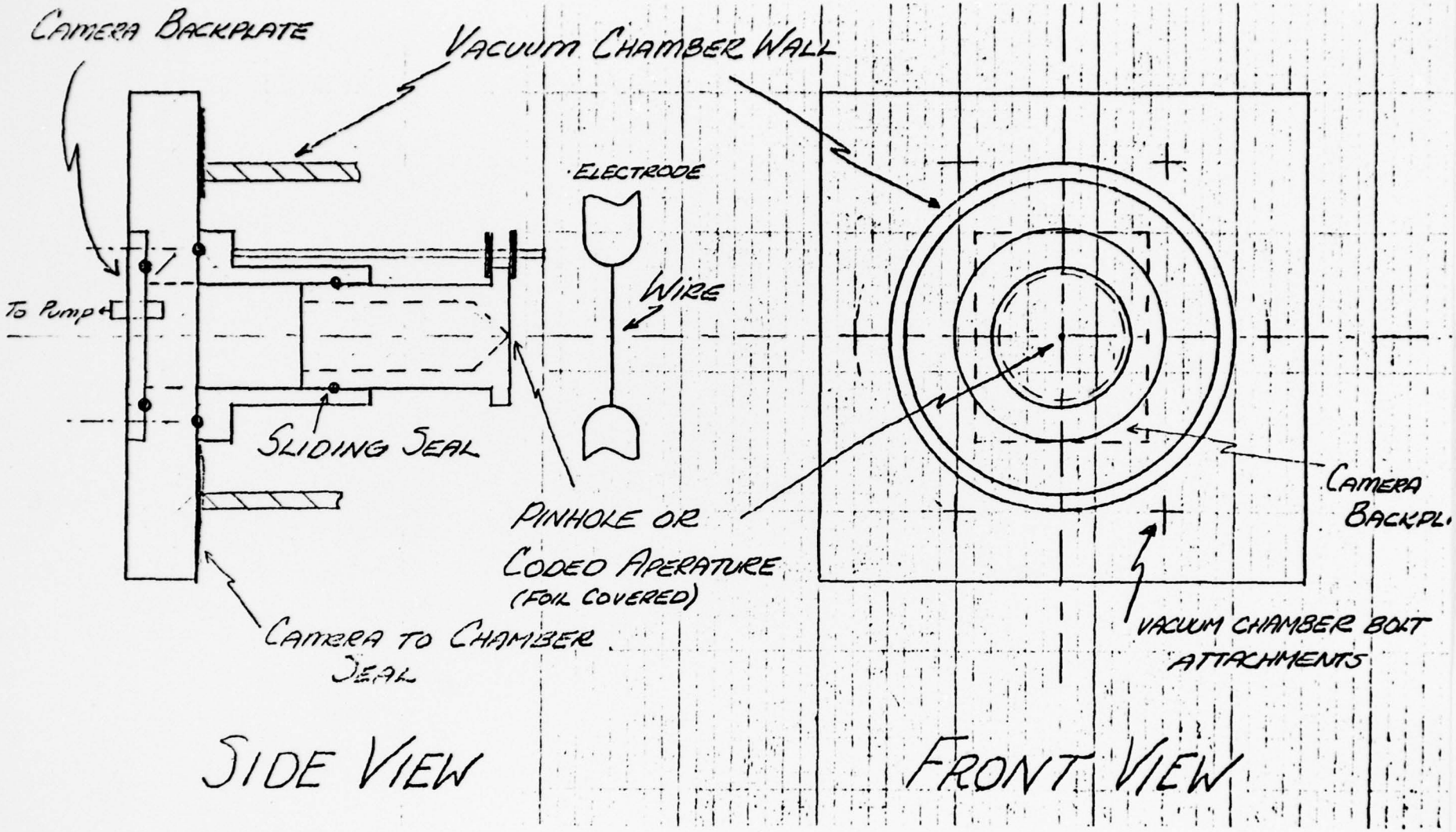

Figure 29. Pinhole Camera.

SECURITY CLASSIFICATION OF THIS PAGE (When Data Entered)

RECEIVED DEC 26 1978

REPORT DOCUMENTATION PAGE

READ INSTRUCTIONS BEFORE COMPLETING FORM

1. REPORT NUMBER: AFOSR-TR-79-0044	2. GOVT ACCESSION NO.
3. RECIPIENT'S CATALOG NUMBER	
4. TITLE (and Subtitle): Laser Diagnostics of Metallic Plasmas	5. TYPE OF REPORT & PERIOD COVERED: Final Report, June 1, 1974 to Oct. 31, 1978
6. PERFORMING ORG. REPORT NUMBER: 1 Jun 74-31 Oct 78	
7. AUTHOR(s): David R. Bach	8. CONTRACT OR GRANT NUMBER(s): AFOSR-74-2713
9. PERFORMING ORGANIZATION NAME AND ADDRESS: University of Michigan, Nuclear Engineering Dept. 2272 GG Brown Laboratory Ann Arbor, Michigan 48109	10. PROGRAM ELEMENT, PROJECT, TASK AREA & WORK UNIT NUMBERS: 61102F 2301/A2
11. CONTROLLING OFFICE NAME AND ADDRESS: Air Force Office of Scientific Research/NP Bldg 410 Bolling AFB, D.C. 20332	12. REPORT DATE: December 1978 13. NUMBER OF PAGES: 60
14. MONITORING AGENCY NAME & ADDRESS (if different from Controlling Office): 65 p.	15. SECURITY CLASS. (of this report): unclassified 15a. DECLASSIFICATION/DOWNGRADING SCHEDULE

16. DISTRIBUTION STATEMENT (of this Report)

Approved for public release; distribution unlimited.

DISTRIBUTION STATEMENT A
Approved for public release; Distribution Unlimited

17. DISTRIBUTION STATEMENT (of the abstract entered in Block 20, if different from Report)

18. SUPPLEMENTARY NOTES

19. KEY WORDS (Continue on reverse side if necessary and identify by block number)

20. ABSTRACT (Continue on reverse side if necessary and identify by block number)

The major objectives of the research described was the study of diagnostic techniques for metallic plasmas produced by exploded wire systems. Work accomplished included the development of a diamond die for the extrusion of lithium, ray tracing calculations to determine the deflection and absorption of rays passing through the plasma, and a transmission line calculation used for the design of etalons. Measurements made include X-ray temperature determinations by the line ratio method using scintillator detectors. Experiments were also carried out on a large area CdS detector for the measurement of infrared radiation.

DD FORM 1 JAN 73 1473 EDITION OF 1 NOV 65 IS OBSOLETE

228 717

unclassified

SECURITY CLASSIFICATION OF THIS PAGE (When Data Entered)

A two-wavelength holographic interferometer was designed, constructed, tested, and used for the measurement of density distribution in the exploded wire plasma and a Z-pinch. The useful measurements were made with the system at the ruby doubled frequency, as the transmission through the plasma was greater at this wavelength.

The exploded wire system has been modified to accept solid wires of tungsten and aluminum which can be fed from outside the vacuum system and a new X-ray measuring system has been constructed.